

# Analysis of two heat storage integrations for an Organic Rankine Cycle

## 2 Parabolic trough solar power plant

R.Chacartegui<sup>a</sup>, Leo Vigna<sup>a,b</sup>, J. A Becerra<sup>a</sup>, V. Verda<sup>b</sup>

4

a Department of Energy Engineering, University of Seville, Spain

6

b. Department of Energy Engineering, Politecnico di Torino, Italy

## 8 ABSTRACT

Among the concentrated solar power technologies, those based on Organic Rankine Cycles  
10 have a very low market presence. However they have favourable characteristics for applications  
with low temperature and small/medium size (<10MW), such as off-grid applications or  
12 distributed power generation.

In this paper is analyzed a 5MW parabolic trough plant integrated with an Organic Rankine  
14 cycle power block and thermal storage. On this purpose, two different thermal storage  
integrations are analysed. They are based on two different heat storage layouts: direct system  
16 using Hitec XL both as Heat Transfer Fluid and as storage medium; indirect system using  
Therminol VP-1 as Heat Transfer Fluid and Hitec XL as storage medium.

18 Full system performance at rated and off-design conditions is presented operating with different  
organic working fluids. Its potential application and main challenges for its development are  
20 discussed in terms of performance and costs. Among the analysed working fluids, the best  
results were obtained for the cycle working with Toluene with an efficiency at the power block  
22 of 31.5% and an estimated power block cost of 825 €/kW. The indirect storage layout was the  
most interesting from the point of view of Levelized Electricity Cost (16.3 c€/kW) and  
24 productivity (28.2 GWh/y for a 5 MW<sub>el</sub> plant) for 10 hours of storage. However, it results in a

storage tanks volume 26% greater than the obtained for the equivalent direct storage layout.

- 2 The results show the competitiveness and the potential of the proposed integrated small size  
parabolic trough designs for isolated applications as mines or for some distributed generation  
4 uses where grid capacity is limited.

## **KEYWORDS**

- 6 Solar energy, Energy Storage, Parabolic Trough Technology, Organic Rankine cycle, ORC,  
CSP.

## **8 1. INTRODUCTION**

Concentrated Solar Power (CSP) technologies are among the renewable technologies with  
10 greater potential for mitigating climate change [1]. They combine flexibility for energy  
generation and capacity for thermal energy storage (TES) to enhance energy supply security  
12 [2]. CSP plants with thermal energy storage can support power generation and provide ancillary  
services including voltage support, frequency response, regulation and spinning reserves, and  
14 ramping serves [3] .In addition, to increase flexibility, CSP plants can also be equipped with  
backup power from combustible fuels to cover demand when solar resource is not available  
16 [4]. In 2012 the global power in CSP plants was 2.7 GW [5] whereas the projects in  
development or under construction will increase the installed CSP capacity in the world up to  
18 15 GW.

Among CSP technologies, parabolic trough collector technology (PTC) has reached the highest  
20 level of commercial maturity and accounts for the largest share of the current CSP market, but  
other technologies at different stages of technology maturity will increase their presence in the  
22 future [6]. A parabolic solar collector consists of a parabolic trough concentrator reflecting  
direct radiation on the focal line of the parabola, where the absorber tube is located. Different  
24 commercial collectors are available e.g. LS-3, EuroTrough and Solar Genix Collector, SENER

[7]. It is the most mature CSP technology due to continuous advances improving the characteristics and performance of the parabolic trough solar collector and its parabolic-shaped reflectors [8]. Different models have been developed to evaluate the cost evolution of the PTC CSP- solar electricity as function of different parameters [9] and to analyse the effects of the economic strategies on CSP plants viability and sizing [10]. The main cost of CSP parabolic trough plants is solar field, with a contribution above 50% of the total investment cost [11]. Current investment costs are estimated in the range between 6600-8688 \$/kWe [11,12] but it is expected that in next decade they will go to values below 6000 \$/kWe by 2020[11,13]. Levelized Cost of Electricity (LCE) of parabolic trough plants is in the range 0.20 -0.33 c\$/kWh at present, depending on their location, whether they include energy storage and the particulars of the project [11, 12]. Perspectives are that PTC-CSP plants will evolve to LCE values below 13 c\$/kWh in future large scale plants [11-13]. Advances for reduction costs in PTC plants are associated to: technology scaling up; solar field massive production with associated cost reduction; high temperature heat transfer fluids; high efficiency power blocks; advances in energy storage [12,14].

As CSP technology, parabolic trough technology allows the possibility to store thermal energy. It involves over-sizing the solar field and increasing the annual utilization factor of the plant. Different technologies [15] and materials [15] for energy storage can be used with different levels of maturity and costs. Most recent commercial CSP plants use molten salts as storage commercial technology [17].

Current large-scale systems rely on traditional well-established steam-based Rankine cycles for power production. Organic Rankine Cycle power plants are an interesting alternative for small-medium plants and relative low temperature heat sources. Fluid characteristics make ORC favourable for applications with medium-low temperature heat recovery [18] (normally less than 400°C), as in the case of parabolic trough solar energy applications. In relative small

power plant sizes ( $<5\text{MW}$ ), adequate for modular solutions, the use of organic working fluids results in a more compact and less costly plant than traditional steam cycle power plants. Steam Rankine cycle operating at moderate temperature and small power ranges would have to use a simple Rankine cycle layout because a regenerative steam turbine would not be not viable for this power size. The simple Rankine cycle would have a similar (or lower ) power block efficiency than the obtained with the equivalent ORC but without the advantages of ORC: modularity and high efficiency at partial load operation.

The use of ORC in CSP plants have been studied in different applications as hybrid systems combined with biomass [19], integrated in CSP tower plants [20,21] or in demonstration pilot plants for analysing the integrated operation [22,23]. ORC plants have good performance at partial loads. Off-design and partial operation of ORC power block has been studied by different authors. In [24] is studied the effect of heat source temperature in cycle's performance, meanwhile in [25] is analysed the off-design operation of a CSP-ORC with compound parabolic collector. In [26] off-design performance analysis of a geothermal ORC is presented based on the preliminary design of turbines and heat exchangers.

Application to mid and small size CSP plants is found in [27] where partial load operation for  $5\text{MW}_{\text{el}}$  indirect ORC cycle coupled to linear solar collectors with different technologies is assessed evaluating the effect of two control strategies on annual electricity output. In this analysis Levelized Electricity Cost value (LEC) was 180-175 €/MWh with sliding pressure off-design control strategy. In [28] is presented a thermodynamic analysis of a micro ORC CSP plant working with different organic fluids. In [29] a dynamic simulation is given for the coupling of solar thermal collectors with a  $6\text{ kW}_{\text{el}}$  ORC, simultaneously producing electric energy and low temperature heat. Besides integration of both technologies is shared with applications for refrigeration as solar heat pumps [30] and combined cooling, heating and power systems (CCHP) [31,32], combined with geothermal [33] or in high efficiency systems

integration for trigeneration [34]. Main challenges for this integration of technologies are the  
2 reduction of investment costs for the whole system and the main components: solar field, heat  
transfer fluid, heat storage system and power block [35].

4 The aim of this paper is the characterization of an ORC parabolic trough power plant of 5MWe  
with two different active storage systems: a) two tanks indirect storage system and b) two tanks  
6 direct storage system. For the analysis of the integration, three organic fluids have been selected  
by considering the temperature range, cycle efficiency, critical temperature and thermal  
8 stability: Toluene, Cyclohexane and siloxane D4. Two Heat Transfer Fluids (HTF) have been  
used: Oil Therminol VP-1 and molten salt Hitec XL [36, 37]. Therminol VP1, used as HTF  
10 fluid in the indirect system, can work in a wider range of temperatures and with slightly higher  
maximum temperatures than other commercial heating oils. For the direct storage system  
12 layout, the use of a molten salt as HTF and storage media allows operating at higher  
temperatures (up to 500°C) and eliminates the need for the oil-to-salt heat exchanger. It allows  
14 a substantial reduction in the costs of TES system, improving the performance of the plant and  
reducing the levelized electrical cost [37]. Hitec XL has been selected because its relatively low  
16 freezing point (120°C).

The structure of this paper is the following. First, the plant layouts and thermodynamic models  
18 of the components are described. Then, these models are used to analyse the effect of main  
design parameters in the two plant configurations and to set the rated operation parameter  
20 criteria. Once the design conditions are established and equipment sized, off-design operation  
is analyzed. Finally, the economic models are described and, with the defined equipment and  
22 operation parameters, economic analyses are developed under the operation criteria. The results  
of the study show the interest of the two storage configurations for small and mid-size power  
24 plants (>5MW).

## 2. CSP system layouts and application framework

2 Solar high temperature storage systems can be classified in active and passive systems. In active  
storage systems, heat is transferred into the storage material by forced convection. The storage  
4 medium itself circulates through a heat exchanger (it can also have other functions as solar  
receiver or a steam generator). This system uses one or two tanks as storage media. Active  
6 systems are subdivided into direct and indirect systems. In a direct system, the heat transfer  
fluid also serves as storage medium, while in an indirect system, a second medium is used for  
8 thermal energy storage. As opposite, the passive storage systems are generally dual medium  
storage systems: the HTF passes through the storage system only for charging and discharging  
10 the storage material. The HTF carries energy received from the energy source to the storage  
medium in the charging phase, and receives energy from the storage when discharging. The  
12 main disadvantage of passive systems is that the HTF temperature decreases during the  
discharging phase as the storage material cools down. In addition, and depending of the system,  
14 heat transfer coefficient is relatively low, and additional heat exchanger are required between  
the HTF and the storage material.

16 This paper analyses the integration of an ORC power block with two different active storage  
systems in a parabolic trough CSP plant, figure 1. These layouts are: a) two tanks indirect  
18 storage system and b) two tanks direct storage system. In [27] an indirect TES system has been  
studied for a 5MWel CSP ORC plant obtaining LCOE values in the range 17.5-18.0 c€/kWh.  
20 This configuration was the selected in [36] for studying the effect of different backup options  
(among them energy storage) and cooling options and LCOE values in the same range. They  
22 can be used with synthetic oils, as in this study, although the use of alternative fluids as nitrogen  
have been proposed [37]. The two tanks direct storage system layout [39] has as main  
24 advantages [40] that cold and heat storage materials are stored separately; low-risk approach;  
possibility to raise the solar field output temperature to 450/500 °C. This technology has been

used in Solar 3 (Fuentes de Andalucia, Seville, Spain) [40]. For reducing storage volume and associated cost, direct thermocline single tank are proposed [39, 41].

For this work these two storage layouts were selected as adequate candidates for the CSP/ORC plant characteristics (temperature range and size). Figure 1 shows the two configurations for the solar power plant under study.

For this study the plant has been located in the province of Seville, at coordinates 37°14'12'' North and 6°1'6'' West, figure 2. Annual sunlight in this location is estimated in 2050 KWh/m<sup>2</sup> [42,43]. The maximum temperature conditioned by the heat transfer fluid properties was set to 400 °C (corresponds to T8 in the solar field, figure 1). The equations that describe the performance of the components of the cycle have been developed in EES [44] and Matlab [45] using a lumped volume method. The resulting coupled system of algebraic equations have been solved to provide a steady state solution for systems sizing at rated conditions. For the defined equipment, performance curves have been estimated in the off-design model and they have been used to simulate plant operation under different operation profiles. As input of the models, Direct Normal Irradiance (DNI) values were used at the reference location with daily data in an interval of 15 minutes [46]. The rated DNI for plant sizing was 700 W/m<sup>2</sup> [43,47].

**Figure 1. PTC/ORC CSP power plants: two tanks direct (a and c) and indirect (b and d) thermal energy storage (TES) system. Direct system: HTF Hitec XL, Storage Medium: Hitec XL. Indirect system HTF: Therminol VP-1, Storage Medium: Hitec XL**

**Figure 2. Direct normal irradiance monthly patterns used for the analyses (left) and CSP plant location (right)**

24

26

## ORC WORKING FLUIDS

### 2 Organic fluids for power cycle

In the ORC power block different design options were considered for the analyses: non-  
4 recuperative cycle/recuperative cycle and saturated/superheated fluid. Detailed discussion  
about ORC working fluids selection and properties can be found in literature for different  
6 applications and temperatures: CSP plants [20,21], use of organic-fluid mixtures [48], use of  
siloxanes [21,49], waste heat recovery [50], high temperature cycles [51] or biomass plants  
8 [52].

For this application, with maximum temperature constrained by the heating oil at 400°C, three  
10 organic fluids have been selected based on their critical temperatures and thermal stability:  
Toluene, Cyclohexane and siloxane D4. Toluene has the highest critical temperature among the  
12 three selected fluids. It does not present thermal stability problems in the range of the  
temperature used in this study [53]. Cyclohexane can also reach high efficiencies [54], but it  
14 features a lower critical temperature than Toluene and presents thermal instability over 288°C.  
Toluene and Cyclohexane, being hydrocarbons, are highly flammable. Finally, the third fluid  
16 used is the siloxane D4. Siloxane (polymethylsiloxanes), or silicon oils, are linear (MM, MDM,  
MD2M) or cyclic polymers (D4, D5, D6) composed of alternating silicone-oxygen atoms with  
18 methyl groups attached to the silicon atoms. In previous works of the authors [20,21, 54] are  
given details of fluids properties and fluid selection for those fluids included in this analysis.  
20 Table 1 shows the main characteristics of the selected organic fluids keeping constant the  
parameter fixed in the solar cycle and the inlet temperature of the heat transfer fluid in the  
22 intermediate heat exchanger constrained by the heating oil stability (400°C). The higher  
molecular weight of these organic fluids results in quite different densities at the inlet and outlet  
24 of the turbine. These fluids have a lower speed of sound than steam, it limits maximum stage  
velocity and expansion ratio and, thus, it can be expected that more turbine stages are needed

compared to a steam turbine. However, if density and specific enthalpy are considered, the estimated size of a vapour turbine with similar power capacity would be 20% smaller for toluene and 16% smaller for cyclohexane related to a reference steam turbine [55]. At turbine outlet Toluene, Cyclohexane and D4 densities after expanding are 0.43, 0.57 and 0.32 kg/m<sup>3</sup> respectively, while steam has a density of 0.05 kg/m<sup>3</sup>. For the selected power plant size, 5MW, no specific problems regarding machinery size are expected although equipment specific design for each working fluid is required.

**Table 1: ORC Working fluids properties**

### **Heat transfer fluid and storage media**

The indirect storage system uses Therminol VP-1 as HTF and Hitec XL as storage media, while the direct storage system uses Hitec XL both as HTF and as storage media. The properties of Therminol VP-1 and Hitec XL have been taken from Solutia data [56] and EES (Engineering Equation Solver) [44]. Their main characteristics are shown in table 2.

Although different oils can be used as HTF, such as Syltherm-800, Downtherm A, Downtherm Q, Caloria HT-43, Therminol VP1 has been selected because it can work at a wider range of temperatures and at slightly higher maximum temperatures than the others. Therminol VP-1, a eutectic mixture of 73.5% diphenyl oxide and 26.5% of diphenyl, has a low freezing point (12°C) and is stable up to 400°C. The vapour pressure of current synthetic or mineral oils exceeds atmospheric pressure at the temperatures required for use as thermal storage media. This would require impractically large pressure vessels, making this alternative unsuitable for direct storage systems [57, 58]. In the direct storage system, molten salts are used as HTF but also as storage media allowing a reduction in TES system cost [59]. On the other hand, molten salts freeze at relatively high temperatures (120–220°C) and special care must be taken to

ensure that the salt does not freeze in the solar field, piping during the night and heating it when  
2 necessary. Up to date, the molten salts most used are Hitec (7% NaNO<sub>3</sub>, 53% KNO<sub>3</sub>, 40%  
KNO<sub>3</sub>), Hitec XL (60% NaNO<sub>3</sub>, 40% KNO<sub>3</sub>) and the so-called Solar Salt (48% Ca(NO<sub>3</sub>)<sub>2</sub>, 7%  
4 NaNO<sub>3</sub>, 45% KNO<sub>3</sub>) [38,60]. Among the mentioned molten salts, Hitec XL features the lower  
freezing point 120°C and similar properties to the others, allowing operating in a wider  
6 temperature range, reducing technical problems and the required energy to keep the salt  
temperature above the freezing point.

8

**Table 2: HTF and storage media properties**

10

### **3 CSP PLANT MODEL**

12 Equations and main assumptions used for the steady state lumped model are described in this  
section. The layouts and points used for the model are presented in figure 1.

#### **14 Solar field.**

The overall efficiency of the collector can be represented as the optical efficiency,  $\eta_0$  minus an  
16 efficiency penalty term,  $\eta'$  representing thermal losses

$$\eta = \eta_0 - \eta' \quad (1)$$

18

$$\eta' = \frac{n q_L}{I_{DN} A_{coll}} \quad (2)$$

Eq. 3 describes the collector efficiency as function of temperatures and irradiance. The curve  
20 comes from National Renewable Energy Laboratory. They tested a SkyTrough collector [61],  
using a Schott PTR80 receiver. The parabolic trough collector efficiency curve has been  
22 generated from separate measurements of outdoor optical efficiency and indoor receiver heat  
loss. Parabolic trough collector efficiency is much more dependent on the operating temperature  
24 than the ambient temperature. In [61] is shown how increasing the ambient test temperature from  
25°C to 40°C decreases the heat loss by 1% and decreasing the ambient temperature to 0°C

increases the heat loss by 2%. For the temperature range on the selected location, and taking into account the coupled efficiency factor, associated heat loss with temperature will typically affects to the global efficiency by a variation lower than 0.2%. Thus, for simulations the ambient temperature has been set at 25°C, neglecting the influence of its variation. Departing from the data presented in [61] curves of different DNI can be collapsed into a single curve for representing the effect of losses with operating temperature. This curve is given in (3):

$$\eta_{coll} = a_1 x^3 + a_2 x^2 - a_3 x + a_4 \quad (3)$$

Where X is defined as:

$$x = \frac{T_{HTF} - T_{amb}}{I_{DN}^{0.33}} \quad (4)$$

$T_{HTF}$  is the heat transfer fluid temperature, calculated as average between the inlet and the outlet temperature:

$$T_{HTF} = \frac{T_7 + T_8}{2} \quad (5)$$

The values of the parameters  $a_1$ ,  $a_2$ ,  $a_3$  and  $a_4$  are respectively:  $-1.26 \times 10^{-6}$ ;  $3.02 \times 10^{-5}$ ;  $6.24 \times 10^{-4}$ ; 0.773.

The collector efficiency can be also expressed as:

$$\eta_{coll} = \frac{\dot{Q}_{solar\_field}}{I_{DN} A_{coll}} \quad (6)$$

In addition, the power collected by the HTF in the solar field can be calculated as

$$\dot{Q}_{solar\_field} = \dot{m}_{HTF} (h_8 - h_7) \quad (7)$$

Solar multiple used in the economic analyses is defined as

$$SM = \frac{\dot{Q}_{solar\_field}}{\dot{Q}_{intermediate\_he}} \quad (8)$$

With  $\dot{Q}_{solar\_field}$  being the rated thermal power collected in the solar field and  $\dot{Q}_{intermediate\_he}$  the rated thermal input of the power block [62].

### **Turbines and pumps**

The electric power absorbed by the pump is given by:

$$P_{el\_pump} = \frac{\dot{m}_{ORC} (h_2 - h_1)}{\eta_{mecc}} \quad (9)$$

2 Electric power generated by the turbine is:

$$P_{el\_turb} = \dot{m}_{ORC} (h_3 - h_4) \eta_{gen} \quad (10)$$

4 The partial load performance of the turbine has been modelled by an equivalent nozzle approximation on the assumption that it works in choked conditions in the entire load range.

6 The isentropic nominal turbine efficiency  $\eta_{is\_turb}$  has been assumed equal to 0.85; the polytropic nominal turbine efficiency  $\eta_{pol\_turb\_nom}$  and the turbine efficiency at partial loads

8 were calculated with equations (11) and (12).

$$\eta_{p\_turb} = \eta_{pol\_turb\_nom} \left( 1 - 0.5 \left( \sqrt{\Delta h_{is\_nom} / \Delta h_{is}} - 1 \right) \right) \quad (11)$$

$$\eta_{is\_turb} = \frac{1 - \left( \frac{1}{r_t} \right)^{\frac{\gamma-1}{\gamma}} \eta_{pol\_turb}}{1 - \left( \frac{1}{r_t} \right)^{\frac{\gamma-1}{\gamma}}} \quad (12)$$

12 Where  $\Delta h_{is\_nom}$  and  $\Delta h_{is}$  are, respectively, the nominal isentropic enthalpy drop and the isentropic enthalpy drop in the turbine;  $r_t$  is the turbine expansion ratio.

### Heat exchangers

14 For modelling this plant, shell-and-tube heat exchangers were adopted. They are used widely in the chemical process industries and in power plants. Heat is transferred from one fluid to the other through the tube walls, either from the tube side to shell or vice versa. The fluids can be either liquids or gases on either the shell or the tube side [63,64]. Heat exchangers have been sized by the log mean temperature difference method (LMTD). The equations that describe the heat released or absorbed by the fluids and the heat transferred across heat exchangers surfaces are given by:

$$Q = C_{hot} * (T_{hot,in} - T_{hot,out}) \quad (13)$$

$$Q = C_{cold} * (T_{cold,out} - T_{cold,in}) \quad (14)$$

$$Q = U \cdot A \cdot \Delta T_{lm} \quad (15)$$

24 The log mean temperature difference  $\Delta T_{lm}$  for countercurrent flow is given by:

$$\Delta T_{lm} = \frac{\Delta T_2 - \Delta T_1}{\ln(\Delta T_2 / \Delta T_1)} \quad (16)$$

2 Where:

$$\Delta T_1 = T_{hot,in} - T_{cold,out} \quad (17)$$

$$\Delta T_2 = T_{hot,out} - T_{cold,in} \quad (18)$$

$$U = \frac{1}{\left(\frac{1}{h_{in}} + \frac{s}{k} + \frac{1}{h_{out}}\right)} \quad (19)$$

6

To calculate the overall heat transfer coefficient U, correlations have been used for determining  
 8 convective heat transfer coefficients and friction losses in the different components of the power  
 block, as function of the characteristics of the streams. For the evaluation of the external fluxes  
 10 in the economizer, in the super-heater, in the recuperator and in the oil-to-salt heat exchanger,  
 the empirical correlation due to Hilpert has been used [65]. For internal flows, considering  
 12 staying in the turbulent and fully developed region it is possible to use the correlation provided  
 by Gnielinski, valid over a large Reynolds number range including the transition region. This  
 14 correlation has been applied to the economizer, superheater, recuperator and oil-to-salt heat  
 exchanger, while, for what concerns the condenser, the convective heat transfer coefficient has  
 16 been calculated through the Chato correlation [66].

Finally, the calculation of the mean convective coefficient along the tube of the evaporator has  
 18 been done as average of calculated values of the convective coefficient at different quality in  
 the tube according to equation (25) [67].

20

**Table 3. Heat transfer correlations used for heat exchangers models**

22

### **Storage Capacity**

The storage capacity is expressed in terms of equivalent operating hours at rated operation with only the thermal energy stored. The volume of the tanks has been calculated through the following formula as function of the storage capacity.

$$V_{tank} = \frac{\dot{m}_{Hitec\_discharging} * n^{\circ} \text{discharging hours} * 3600}{\rho_9} \quad (26)$$

Where  $\rho_9$  is the density in the hot tank. In the analyses, the storage capacity varies between no storage and 10 operating hours [68,69].

## ANALYSIS OF THE DESIGN OPERATION OF THE CYCLE

In this section analyses on cycle design and operation are shown to identify the effect of main design parameters on the plant performance for the different layouts. As a general rule of thumb, the maximum evaporation temperature for each fluid has been set to 10 °C lower than the critical temperature. Toluene and Cyclohexane have higher evaporation pressures than D4. Toluene's condensation pressure is very similar to the equivalent steam cycle condensation pressure for the range of analysis, while Cyclohexane and D4 have higher pressures of condensation than Toluene and steam. Siloxane D4 presents the highest condensation temperature. Main data used for the analyses are shown in table 4.

### Table 4: Power plant main assumptions

#### Power block analysis

##### Rated conditions

To set power block design conditions different analyses were performed to identify the effect of design parameters in the performance of the cycle with the different working fluids. For power block design evaporation and condensation temperatures are analysed as in [29] or [55]. Figure 3 shows the efficiency of the power block as function of evaporation temperature (left)

and condensation temperature (right) for each organic fluid. On the left side, for each fluid, condensation temperature has been fixed (60°C Toluene, 40°C Cyclohexane 87°C for D4). Results for both recuperative and non-recuperative layouts are shown in figure 3. Figure 3 shows how Toluene has the highest efficiency, toluene's non-recuperative layout efficiency is close to 22%. The recuperative layout has a different impact depending on the working fluid, it gives an average increase of 9%, 4.3% and 4% for D4, Cyclohexane and Toluene respectively. The greater increase with D4 is due to its positive saturation vapour curve with a very small slope that results in a greater capacity of heat recovery. Figure 3 (right) shows the influence of condensation pressure on the power block efficiency. These analyses have been done by setting the evaporation temperature at 302°C for Toluene, at 265°C for Cyclohexane and at 307°C for D4. Efficiency decreases with the increase of the condensation temperature. Condensation pressure is directly linked to condenser characteristics and its heat evacuation capacity. In PTC-ORC CSP applications condenser temperature variations between 20-40°C can be expected, what is reflected in a efficiency penalty associated to condenser temperature up to 3% depending on the operating conditions. This effect is bigger on the recuperative layout because of the double effect on reduction of turbine expansion and heat recovery capacity at the recuperator. For the condensation temperature range (constrained by the minimum acceptable condenser pressure) the efficiency decreases 4.4% for Toluene, 5.3% for Cyclohexane and 3.4% for D4.

20

**Figure 3: Power block efficiency as function of the evaporation temperature for recuperative and non-recuperative cycles (left). Condensation pressure effect on recuperative cycle efficiency (right).**

24 The selection of condenser pressure affects to the sizing of equipment and associated costs. In table 5, is shown the effect of the variation of condenser pressure in toluene's heat exchangers

design. The global heat transfer coefficient in the recuperator ( $U_{rec}$ ) is very low due to the convective coefficient of the vapor side in the recuperator. Increasing ( $U_{rec}$ ) raises directly affects to the heat transfer area and recuperator cost. The variation of the condensation pressure has a lower influence on the global heat transfer coefficient of the condenser. As in the condenser there is a two-phase flow, liquid phase improves considerably the average convective coefficient of the organic fluids.

### 8 **Table 5. Influence of condensation pressure on Toluene's heat exchangers design**

10 At constant pressure, superheating penalizes the efficiency of the non-recuperative cycle due to the convergent evolution of isobars for increasing entropy in the gas region of T-s diagram  
12 [20,21]. However, the use of superheating can reduce the mass flows required in the solar and storage systems, reducing the equipment costs although with an efficiency decrease. This is  
14 specially relevant for D4 with a mass flow three times bigger than for Toluene and Cyclohexane. In table 6 are presented the selected design conditions for the ORC power block after the  
16 analyses. The temperature of condensation was selected in a compromise between cost (heat exchangers areas), performance and pressure technical limit. The rated condensation  
18 temperatures are 55°C, 40°C and 87°C for toluene, Cyclohexane and D4. D4 has the lowest condensation pressure (0.049 bar), while toluene condenses at 0.151 bar and Cyclohexane at  
20 0.245 bar. The evaporation temperature has been chosen according to the analysis of the effect of superheating on the cycle efficiency and plant costs, given that, for Cyclohexane and D4, the  
22 temperature at the turbine inlet  $T_3$  is limited by the thermal stability of these fluids [53, 55]. These evaporation pressures are clearly lower than the water evaporation pressure in the same  
24 temperature range (80-100 bars). It benefits heat exchanger design and cost, reduced thickness pipes and cheaper materials can be used in the intermediate heat exchanger.

26

**Table 6. ORC costs, efficiencies and mass flow (5 MW<sub>el</sub> plant)**

2

In table 7 the overall results for the 5MW power block with these parameters are shown. For what concern the efficiency and the power block cost, recuperative Toluene appears as the best solution. It has a good efficiency for this size of power plant, 31.5%, and the estimated power block cost is 825 €/kW<sub>el</sub> (next section explain the economic assumptions) Cyclohexane also presents a good efficiency (28.7%) and a slightly higher cost (933 €/kW<sub>el</sub>). D4 is the worst solution for this kind of plant: its efficiency is 23.4% and the cost is clearly higher 1088 €/kW<sub>el</sub>. D4 has a high temperature of condensation, which negatively influences its performance. On the other hand, this characteristic could be suitable for other applications, as cooling using an absorption cycle. In fact, for condensation temperature in the range 90-130°C D4 features higher efficiencies than Toluene and Cyclohexane.

Table 7 shows the design conditions for the solar cycle for the different organic fluid cases. These results do not include the thermal storage systems (SM=1). For what concerns the indirect system case, when the thermal storage system will be taken into account, temperatures T<sub>6</sub> and T<sub>7</sub> will change (figure 1), being T<sub>6</sub> the result of a mix between the mass flow coming from the intermediate heat exchanger and the mass flow coming from the oil-to-salt heat exchanger. In Table 7 are shown the HTF mass flows in the intermediate heat exchanger. The Hitec XL mass flows (direct system) are higher than Therminol V-1 mass flows. This is due to the difference of specific heat of the two heat transfer fluids used. At 300°C The specific heat of Therminol VP-1 and Hitec XL are 2318 KJ/(kg K) and 1447 KJ/(kg K), respectively. The Cyclohexane cases present the lowest HTF fluid mass flow in both cases, since the temperature drop in the intermediate heat exchanger for Cyclohexane cases is higher.

24

**Table 7. PTC/ORC design conditions (5 MW<sub>el</sub> plant)**

Plant efficiency is the combined effect of the ORC efficiency trends and heat exchange efficiency that is evaluated from heat exchanger T-Q diagrams. Considering a DNI of 700 W/m<sup>2</sup>, the global plant efficiency with Toluene is 23.6%, with Cyclohexane 21.6% and with D4 is 17.3%. With the storage system, and a solar multiple greater than 1, higher mass flows will be needed for the storage system and clear differences between direct and indirect systems will appear.

Figure 4 shows the intermediate heat exchanger T-Q diagrams for the three organic fluids and both storage systems, while in table 6 the inlet and outlet temperatures in the discharging stage of Therminol VP-1 (indirect system) and Hitec XL (direct system) are reported. Heat transfer in the intermediate heat exchanger has been solved by the  $\Delta T_{\min}$  method. For toluene in both cases, for the organic fluid side, the pinch point is at the evaporator inlet. However, using D4 as organic fluid the pinch point is at D4 economizer inlet both in direct and indirect systems. While for Toluene and D4 the pinch point position is the same in both storage system configurations, for Cyclohexane the situation is different: in the indirect system case (Therminol VP-1 as HTF) the pinch point is at the economizer inlet whereas in the direct system case (Hitec XL as HTF) temperature has been set to 200°C in order to maintain the outlet temperature above the safety limit for avoiding Hitec XL freezing (Hitec XL freezing point is 120°C).

**Figure 4: Intermediate HE T-Q diagrams for Toluene (top) Cyclohexane (middle) and D4 (bottom)**

## **Discharging phase – tanks volume**

During the discharging phase the power block works at nominal power. Thus, the organic fluid conditions in the intermediate heat exchanger are those under rated operation. Instead, for what concern the HTF side, there are two cases, depending on the TES configuration: in the direct

system case, the Hitec XL temperatures and mass flow are the same, while in the indirect system case the Therminol VP-1 temperatures and mass flow are different due to heat exchanging in the oil-to-salt heat exchanger.

Temperatures in the storage tanks depend on the organic working fluid, Hitec XL freezing point and storage system layout. Table 8 shows temperatures in the storage tanks and mass flows during the discharging phase for direct and indirect layouts.

#### 8 **Table 8: Direct system and Indirect System – Discharging phase**

10 For each layout, tank volumes have been calculated by evaluating the storage medium volumes needed for providing the thermal energy for the required numbers of hours (storage capacity),  
12 assuming that the power block works at rated conditions during the discharging phase. The maximum range of operation only with the storage system has been set to 10 hours.

14 Figure 5 shows the estimated storage system costs for each case as function of the storage capacity. Direct storage system presents lower costs of the thermal energy storage system, for  
16 cyclohexane and toluene, since temperature differences between tanks are higher and the use of the oil-to-salt heat exchanger is avoided, reducing the cost and the complexity of the system.

18

#### **Figure 5. Thermal Energy Storage System Costs**

20

#### **Off-design conditions. Power block partial load operation**

22 At off-design operation, sliding pressure regulation has been used for the ORC turbine [27].  
The minimum partial load operation for the organic Rankine cycle has been assumed at 25% of  
24 the rated power, 1.25 MW. Stable operation at this partial load can be reached by small ORC plants. At minimum load, mass flow is 30% of the rated operation value.

2 **Figure 6. ORCs evaporation temperature and pressure as function of power plant load**

4 Figure 6 shows the variation of pressure and temperature of evaporation of the three fluids as  
function of power load. At rated conditions, Toluene evaporates at 33.5 bar and 302 °C, while  
6 at minimum load it evaporates at 233 °C and 12.9 bar. Cyclohexane in rated operation  
evaporates at 29,5 bar and 255 °C, while at minimum load it evaporates at 194 °C and 12.1 bar.  
8 Rated conditions for D4 are 11.3 bar and 302°C, whilst at the 25% nominal electric power it is  
regulated at 4.9 bar and 250°C.

10

**Figure 7. Power block efficiency (left) and efficiency/rated capacity efficiency (right) at  
12 partial load**

In figure 7 are given the ORC efficiencies (left) and the rate between the partial load efficiency  
14 and the rated capacity efficiency of the cycle (right). The ORC cycles with Toluene and  
Cyclohexane maintain 90% of rated cycle efficiency down to 50% load. At partial load, D4  
16 maintains efficiency values above 90% of rated efficiency down to 35% load. Under these  
values the cycle efficiencies is subjected to a relatively consistent drop. These high values at  
18 partial load are due to the effect of recuperator that at partial loads improves its efficiency  
compensating partially reducing the penalty on cycle efficiency due to the penalty in turbine  
20 expansion.

**ECONOMIC ANALYSIS**

22 **Economic model**

The capital cost of each heat exchanger has been determined by means of the following  
24 correlations [70].

$$\ln C_p = K_1 + K_2 \ln A + K_3 (\ln A)^2 \quad (27)$$

$$\ln F_p = C_1 + C_2 \ln P + C_3 (\ln P)^2 \quad (28)$$

$$C_{BM} = C_p F_{BM} = C_p (B_1 + B_2 F_M F_p) \quad (29)$$

$$C_{HE} = C_{BM,e} CEPCI_{2014} / CEPCI_{1996} \quad (30)$$

$C_p$  is the basic cost of equipment assuming ambient operating pressure and carbon steel construction in the year of 1996. Fixed head stainless steel shell and tube heat exchangers have been chosen and the operating pressure is higher than the ambient pressure in almost all of the heat exchangers. Therefore, the basic cost  $C_p$  is corrected for the chosen material and for the working pressures by the equations (27,28).  $C_{BM}$  is the corrected cost. The cost of heat exchangers is actualized from 1996 to 2014 costs, using Chemical Engineering Plant Cost Index (CEPCI) values. So  $C_{HE}$  represents the capital cost for heat exchangers and it is expressed in US\$. An exchange rate of 1.26 \$/€ has been used for dollars to euros conversion.  $A$  is the heat transfer area of the heat exchanger and  $P$  the operating pressure expressed in  $m^2$  and kPa. The  $B_i$  ( $i=1,2$ ),  $K_i$ ,  $C_i$  ( $i=1,2,3$ ),  $F_M$ ,  $CEPCI_{1996}$  and  $CEPCI_{2014}$  are the coefficients required for cost evaluation of each equipment. Their values are listed in table 9.

### Table 9: Cost evaluation coefficients

The cost of the turbine thermal machine has been assumed equal to 450 €/kW [71]. This value has been considered the same for the three working fluids. There will a variation in the designs and associated costs with the working fluid however as toluene and cyclohexane sizes are expected to be similar, similar costs are expected, whereas D4 turbine would have a different size and it is expected to have a higher cost. As a preliminary approach, costs difference has been associated to heat exchange area in the different components of the power block. It results in estimated power block cost of 825 €/kW<sub>el</sub> for toluene, 933 €/kW<sub>el</sub> for cyclohexane and 1088

€/kWh<sub>el</sub> for D4. In case of two tanks indirect system the cost of TES also includes the cost of  
 2 the oil-to-salt heat exchanger. The *solar field costs*  $C_{SF}$  that can be found in literature vary from  
 190 and 220 €/m<sup>2</sup>. A conservative approach has been done and a value of 213 €/m<sup>2</sup> has been  
 4 adopted [62]. In table 10 the unit costs used in the economic model are reported. The *thermal  
 storage system cost* has been calculated as sum of two components. One regards the cost of the  
 6 storage medium, whilst the other one regards the equipment costs, expressed by unit of thermal  
 energy stored. The *cost of Hitec XL* is 1.19 \$/kg and the *storage system cost* using HITEC XL  
 8 is 20.1 \$/kWh<sub>t</sub>, whereas the *Therminol VP-1* cost is 2.2 \$/kg and the *storage system cost* is 57.5  
 \$/kWh<sub>t</sub> [38]. The cost expressed in terms of kWh<sub>t</sub> includes costs of tanks, support and  
 10 foundation, electrical and instrumentation, pipes, valves etc. [72]. The higher cost of Therminol  
 VP-1 is due to the need for a pressurized N<sub>2</sub> in the thermal storage tank in order to keep the  
 12 HTF in liquid form. In case of two tanks indirect system configuration the oil-to-salt heat  
 exchanger cost is included in the thermal storage system cost. The total cost of the plant is  
 14 scaled up by 5% in order to take into account the balance-of-plant costs (auxiliary equipment,  
 labours, etc.) [73].

16

**Table 10: Global costs of main elements**

18

The total capital cost  $C_{PL}$  of the plant is:

$$20 \quad C_{PL} = C_{PB} + C_{TES} + C_{SF} + C_{IND} \quad (31)$$

22 The Levelized Energy Cost (LEC), is the minimum price at which energy must be sold for an  
 energy project to break even over the lifetime of the project. It is an economic assessment of  
 24 the cost of the energy-generating system including all the costs over its lifetime: initial  
 investment, operations and maintenance, cost of capital.

The annuity (investment expenditures in a year) has been calculated with an interest rate  $i$  of

2 10% and a number of years  $n$  equal to 20 (life of the system), using the following formula:

$$I = C_{PL} \frac{i(1+i)^n}{(1+i)^n - 1} \quad (32)$$

4 With the initial capital cost, the annuity, the O&M cost and the electricity production over a year it is possible to calculate the Levelized Cost of Electricity (€/kWh).

$$6 \quad LEC = \frac{\sum_{t=1}^n \frac{I_t + O\&M_t + F_t}{(1+i)^t}}{\sum_{t=1}^n \frac{E_t}{(1+i)^t}} \quad (33)$$

Where:

8  $I_t$ : Investment expenditures in the year  $t$

$O\&M_t$ : O&M expenditures in the year  $t$

10  $E_t$ : Electricity generation in the year  $t$

$i$ : Discount rate

12  $n$ : Life of the system

14 The operating and maintenance costs of CSP plants are low compared to fossil fuel power plants, but are still significant. The replacement of receiver mirrors, due to glass breakage, are  
16 significant components of the O&M costs as well as cost of mirror washing, including water costs. Plant insurance is also an important expense and the annual cost for this can be between  
18 0.5%-1% of the initial capital cost. It is currently estimated that a parabolic trough system would have O&M costs including insurance between 0.020 and 0.040 \$/kWh. In order to estimate the  
20 LEC an O&M and insurance cost equal to 0.035 \$/kWh (0.027 €/kWh) have been chosen [12].

## 22 **Superheating effect on plant cost**

As aforementioned, superheating brings relevant benefits in terms of plant cost, reducing heat  
24 exchangers area, although for a given pressure superheating penalizes efficiency in the non-

recuperative cycle [55]. In table 11 the effect of superheating on the different item costs of the plant are shown.

#### **Table 11: Effect of Superheating in the costs of the plant**

Superheating allows to decrease the HTF mass flows required for a given heat exchange. It results in smaller solar field areas, heat exchangers area and thermal storage tanks. The percentage of the savings associated to the system and the CSP power plant are given in table 10. Superheating brings a little improvement for what concern the cost of the power block, but an important reduction of the solar field cost, that roughly corresponds to the 50% of the plant cost.

#### **Storage effect**

Table 12 shows the effect of the storage capacity on the LEC and the directly associated SM [36,47]. For each storage capacity, the optimal solar multiple that minimizes the LEC over a year is reported. The maximum optimal solar multiple obtained from the analysis is 2.5, corresponding with a storage capacity of 10 hours. The levelized electricity cost for a plant with indirect storage system and Toluene is 16 c€/kWh; with Cyclohexane it is slightly higher, 16.7 c€/kWh. In D4 cases the levelized cost of electricity energy is relatively higher, more than 20 cents of €/kWh. The optimum values for the direct TES layouts show slightly higher LEC values than the indirect TES case varying the increase above the optimum result for indirect layout between 0.79 and 1.1 €/kWh.

#### **Table 12: Optimum LEC results as function of storage capacity**

The use of Hitec XL as heat transfer fluid without using its good properties as storage medium brings only higher cost and technical problems (high freezing point). Therminol VP-1 is more suitable for a plant without thermal storage.

**Figure 8. Solar Multiple Effect on LEC for different storage capacities. TES indirect system (left). TES direct system (right).**

In figure 8 is shown LCE's dependency with SM and the storage capacity. The minimum of each curve individuates the optimal Solar Multiple for each storage capacity that minimizes the LEC and it is displaced for each storage capacity. A summary of main results for different storage capacities is given in Table 13. The use of a thermal storage system allows reaching high utilization factors; up to 64.4 % for plants with a 10 hours storage capacity. In addition, with higher storage capacities, the capability to generate electricity according to the demand drastically increases. The electricity production in the case of indirect storage system is slightly higher. The direct system annual electricity productions have been penalized in order to consider the consumed energy for keeping Hitec XL temperature above the safety limit (200°C). According to [74] a thermal storage capacity of 1h is enough for Hitec XL freeze protection operation during the night. Then, based on [74] and by adopting a conservative approach, the direct system annual electricity productions have been penalized by 2% associated to this non used capacity.

**Table 13. Summary of Indirect/Direct TES parabolic trough plant with Toluene as working fluid data**

Figure 9 shows the electricity production, the plant cost and the levelized energy cost as function of the solar multiple for the 6 hours storage capacity. Production and cost curves are normalized on the values that they assume for a SM of 1.25. The production curve shows how production trend changes for solar multiples higher than 2.25. The minimum LEC point corresponds to the solar multiple with a greater difference between the cost curve and the production curve.

**Figure 9. Electricity production, plant cost and LEC as function of SM. TES indirect system (left). TES direct system (right).**

10

Figure 10 shows as function of the Solar Multiple the electricity generated and the relative investment costs of the different parts of the plant. The investment cost for these kind of 5 MW parabolic trough solar plants is between 3800 and 8200 €/kW, considering a storage capacity of 6 hours. The investment cost for plants with direct storage system is slightly lower than the investment cost for plants with indirect storage system. These values are fully competitive compared with the current ones presented in references [11-14] although slightly higher than those expected for next decade. The analysis of the integration taking into account solar field and heat exchangers costs is shown as an adequate strategy for the selection of the optimum energy storage capacity. The solar field is the most expensive part of plant, and its dimensions have a big influence on the resulting levelized cost of energy. The weight of the solar field on the total cost in these analyses varies between 43% and 63%.

22

**Figure 10. Annual electricity production as function of SM (above). Plant investment cost as function of SM (below). TES indirect system (left). TES direct system (right).**

24

## CONCLUSIONS

2 The main conclusions obtained from the analysis are:

- 4 • Toluene appears as the best organic fluid, presenting the best ORC performance (31.5%)  
and the lowest cost (825 €/kW<sub>el</sub>). Furthermore, it has not thermal stability limits in the  
considered temperature range.
- 6 • Cyclohexane also presents a respectable efficiency (28.7%) and a slightly higher cost  
(933 €/kW<sub>el</sub>); it features thermal instability over 288°C.
- 8 • The siloxane D4 shows the worst results: an efficiency of 23.4% and an ORC cost of  
1088 €/kW<sub>el</sub>. Its high condensation temperature (87°C) negatively affects its  
10 performance. On the other hand, this characteristic could be suitable for other  
applications, as cogeneration or trigeneration using an absorption cycle. In fact, for  
12 condensation temperature in the range 90-130°C D4 features higher efficiencies than  
Toluene and Cyclohexane.
- 14 • The temperature of condensation strongly influences performances and costs, in  
particular the size of heat transfer areas and so the cost of one of the most expensive  
16 components of the power block, the recuperator.
- Superheating is a good choice for organic Rankine cycles in solar plants. Actually, it  
18 shows benefits both in terms of performance and in terms of plant costs. Using  
superheating a reduction of the plant cost of about 5-10% is achieved, thanks mainly to  
20 a substantial solar field area reduction.
- The plants with a direct storage system show a slightly lower investment cost than plants  
22 with an indirect storage system. The investment cost for these kinds ORC parabolic  
trough solar power plants with thermal energy storage is between 3500 €/kW (2 hours  
24 storage capacity) and 8500 €/kW (10 hours storage capacity). Approximately the 50%

of the total cost is due to the solar field. These are competitive values compared with the existing in current commercial parabolic trough plants.

- The investment cost for direct thermal energy storage systems is a 17% lower than the investment cost for indirect storage system. Direct TESS figures lower tanks volume and allows avoiding the use of a heat exchanger between the HTF and the storage media.
- Although CSP plants with thermal energy storage have higher specific investment costs due to the storage system and the larger solar field, the greater electricity generation results in a lower electricity generation cost. With thermal energy storage systems high utilization factors (up to 60 % for plants with 10 hours storage capacity) are reached.
- The resulting LEC for the analyzed ORC solar power plants is 16.36-17 c€/kWh with Toluene and Cyclohexane as ORC working fluid and approximately 20 c€/kWh with siloxane D4 as working fluid. These values are in agreement with current LCE of commercial parabolic trough technology Given that parabolic trough technology utilizes standard industrial manufacturing processes, materials, and power cycle equipment, the technology is poised for rapid deployment should the need arise for a low-cost solar power option. ..
- The analyzed 5MW power plant, with LCE 16.3 c€/kWh can be fully competitive with other generation technologies as in the cases of remote off-grid mines or in locations with limited grid capacity where other technologies have relevant fuel transport costs.

## 20 NOMENCLATURE

22	$T_1$ :	Temperature of condensation
	$T_{evap}$ :	Temperature of evaporation
24	$\Delta T_{sh}$ :	$\Delta T$ of superheating
	$T_{w\_in}$ :	Inlet cooling water temperature used in the condenser

	$T_8$ :	solar field HTF outlet temperature
2	$\eta_{is\_pump}$ :	Isentropic pump efficiency
	$\eta_{is\_turb}$ :	Isentropic turbine efficiency.
4	$\eta_{gen}$ :	Generator efficiency
	$P_{el}$ :	Net electric power
6	$\varepsilon_{reg}$ :	Recuperator efficiency
	$\Delta T_{min}$ :	Minimum $\Delta T$ in the heat exchangers, pinch point
8	Coll:	Collector
	CSP:	Concentrated solar power
10	DNI:	Direct normal irradiance
	HTF:	Heat transfer fluid
12	LEC/LCOE:	Levelized Energy Cost
	LMTD:	Log mean temperature difference method
14	ORC:	Organic Rankine Cycle
	PB:	Power block
16	PTC:	Parabolic Trough Collector
	REC:	Recuperative
18	SH:	Superheating
	SM:	Solar multiple
20	TES:	Thermal energy storage

## REFERENCES

- 22 1. International Energy Agency: [www.iea.org/](http://www.iea.org/) Accessed on May 2015
- 24 2. Denholm, P., & Mehos, M. (2014). Enabling greater penetration of solar power via the use of CSP with thermal energy storage. *Solar Energy: Application, Economics, and Public Perception*, 99.

3. J. Forrester, The Value of CSP with Thermal Energy Storage in Providing Grid Stability,  
2 Energy Procedia 49, 2014, 1632-1641
4. Concentrating Solar Power Technology: Principles, Developments and Applications,  
4 Edited by K Lovegrove, W Stei, 2012
5. [www.nrel.gov/csp/solarpaces/operational.cfm](http://www.nrel.gov/csp/solarpaces/operational.cfm) Accessed on May 2015
6. Tomislav M. Pavlovi, Ivana S. Radonj, Dragana D. Milosavljevi, Lana S. Panti, A review of  
6 concentrating solar power plants in the world and their potential use in Serbia, Renewable and  
8 Sustainable Energy Reviews 16 (2012) 3891– 3902
7. Hank Price, Eckhard Lüpfer, David Kearney, Eduardo Zarza, Gilbert Cohen, Randy Gee,  
10 Rod Mahoney, Advances in Parabolic Trough Solar Power Technology, ASME Vol. 124, MAY  
2002.
- 12 8. A. Fernandez-Garcia, E. Zarza, L. Valenzuela, M. Perez, Parabolic-trough solar collectors  
and their applications, Renewable and Sustainable Energy Reviews 14 (2010) 1695–1721.
- 14 9. Hernández-Moro, J., Martínez-Duart, J.M., Guerrero-Lemus, R. , Main parameters  
influencing present solar electricity costs and their evolution (2012-2050), Journal of  
16 Renewable and Sustainable Energy 5, 2013.
10. Sánchez, D. , Frej, H., Muñoz De Escalona, J.M. , Chacartegui, R. , Sánchez, Preferred  
18 plant size of parabolic trough csp power plants, Proceedings of the ASME Turbo Expo 3, 2011,  
1053-1062.
- 20 11. Jim Hinkley, Bryan Curtin, Jenny Hayward, Alex Wonhas (CSIRO) Rod Boyd, Charles  
Grima, Amir Tadros, Ross Hall, Kevin Naicker, Adeb Mikhael, Concentrating solar power –  
22 drivers and opportunities for cost-competitive electricity, 2011.
12. IRENA, Renewable Energy Technologies: Cost Analysis Series, Concentrating Solar  
24 Power, 2012

13. Turchi, C. S. (2010). Parabolic trough reference plant for cost modeling with the solar advisor model (SAM). National Renewable Energy Laboratory.
14. Price, H., & Kearney, D. (2003, January). Reducing the cost of energy from parabolic trough solar power plants. In *ASME 2003 International Solar Energy Conference* (pp. 591-599). American Society of Mechanical Engineers.
15. Zalba, B., Marín, J.M., Cabeza, L.F., Mehling, H., Review on thermal energy storage with phase change: Materials, heat transfer analysis and applications, *Applied Thermal Engineering* 23, 2003, 251-283.
16. Sarada Kuravi, Jamie Trahan, D. Yogi Goswami, Muhammad M. Rahman, Elias K. Stefanakos, Thermal energy storage technologies and systems for concentrating solar power plants, *Progress in Energy and Combustion Science*, Volume 39, Issue 4, August 2013, Pages 285-319
17. Murat Kenisarin, Khamid Mahkamov, Solar energy storage using phase change materials, *Renewable and Sustainable Energy Reviews* 11, 2007, 1913–1965.
18. Hua Tian, Gequn Shu, Haiqiao Wei, Xingyu Liang, Lina Liu, Fluids and parameters optimization for the organic Rankine cycles (ORCs) used in exhaust heat recovery of Internal Combustion Engine (ICE), *Energy* 47 (2012) 125-136.
19. R. Sterrer, S. Schidler, O. Schwandt, P. Franz, A. Hammerschmid, Theoretical Analysis of the Combination of CSP with a Biomass CHP-plant Using ORC-technology in Central Europe, *Energy Procedia* 49 (2014) 1218–1227
20. Chacartegui, R., Muñoz De Escalona, J.M., Sánchez, D., Monje, B., Sánchez, T. 2011, "Alternative cycles based on carbon dioxide for central receiver solar power plants", *Applied Thermal Engineering*, vol. 31, no. 5, pp. 872-879.

21. Sánchez, D., Brenes, B. M., Muñoz de Escalona, J. M. and Chacartegui, R. (2013), Non-  
2 conventional combined cycle for intermediate temperature systems. *Int. J. Energy Res.*, 37:  
403–411
- 4 22. Jonathan R. Raush, Terrence L. Chambers, Ben Russo, Kenneth A. Ritter III,  
Demonstration of Pilot Scale Large Aperture Parabolic Trough Organic Rankine Cycle Solar  
6 Thermal Power Plant in Louisiana, *Journal of Power and Energy Engineering* 1 (2013) 29-39  
23 Chambers, T., Raush, J., Russo, B., Installation and operation of parabolic trough organic  
8 Rankine cycle solar thermal power plant in South Louisiana, *Energy Procedia* 49, 2013, 1107-  
1116.
- 10 24. Fu, B.-R. , Hsu, S.-W., Lee, Y.-R., Hsieh, J.-C., Chang, C.-M., Liu, C.-H., Effect of off-  
design heat source temperature on heat transfer characteristics and system performance of a  
12 250-kW organic Rankine cycle system, *Applied Thermal Engineering* 70, 2014, 7-  
25. Jiangfeng Wang, Zhequan Yan, Pan Zhao, Yiping Dai, Off-design performance analysis of  
14 a solar-powered organic Rankine cycle, *Energy Conversion and Management*, Volume 80,  
April 2014, Pages 150-157.
- 16 26. Dongshuai Hu, Saili Li, Ya Zheng, Jiangfeng Wang, Yiping Dai, Preliminary design and  
off-design performance analysis of an Organic Rankine Cycle for geothermal sources, *Energy*  
18 *Conversion and Management*, Volume 96, 15 May 2015, Pages 175-187.
- 20 27. D. Casartelli, M. Binotti, P. Silva, E. Macchi, E. Roccaro, T. Passera, Power Block Off-  
design Control Strategies for Indirect Solar ORC Cycles, *Energy Procedia*, Volume 69, May  
2015, Pages 1220-1230.
- 22 28. F. Ferrara, A. Gimelli, A. Luongo, Small-scale Concentrated Solar Power (CSP) Plant:  
ORCs Comparison for Different Organic Fluids, *Energy Procedia*, Volume 45, 2014, Pages  
24 217-226.

- 29 Francesco Calise, Massimo Dentice d'Accadia, Maria Vicidomini, Marco Scarpellino,  
2 Design and simulation of a prototype of a small-scale solar CHP system based on evacuated  
flat-plate solar collectors and Organic Rankine Cycle, *Energy Conversion and Management*,  
4 Volume 90, 15 January 2015, Pages 347-363.
- 30.Stefan Schimpf, Roland Span, Techno-economic evaluation of a solar assisted combined  
6 heat pump – Organic Rankine Cycle system, *Energy Conversion and Management*, Volume  
94, April 2015, Pages 430-437.
- 8 31 Fateme Ahmadi Boyaghchi, Parisa Heidarnjad, Thermoeconomic assessment and multi  
objective optimization of a solar micro CCHP based on Organic Rankine Cycle for domestic  
10 application, *Energy Conversion and Management*, Volume 97, June 2015, Pages 224-234.
- 32.Man Wang, Jiangfeng Wang, Pan Zhao, Yiping Dai, Multi-objective optimization of a  
12 combined cooling, heating and power system driven by solar energy, *Energy Conversion and  
Management*, Volume 89, 1 January 2015, Pages 289-297.
- 14 33.Ruzzenenti, F., Bravi, M., Tempesti, D., Salvatici, E., Manfrida, G., & Basosi, R. (2014).  
Evaluation of the environmental sustainability of a micro CHP system fueled by low-  
16 temperature geothermal and solar energy. *Energy Conversion and Management*, 78, 611-616.
- 34.Fahad A. Al-Sulaiman, Ibrahim Dincer, Feridun Hamdullahpur, Thermoeconomic  
18 optimization of three trigeneration systems using organic Rankine cycles: Part II –  
Applications, *Energy Conversion and Management*, Volume 69, May 2013, Pages 209-216.
- 20 35.Quoilin S, Orosz M, Lemort V. Performance and design optimization of a low-cost solar  
Organic Rankine Cycle for remote power generation. *Solar Energy* 2011.
- 22 36.Klein, S.J.W, Multi-criteria decision analysis of concentrated solar power with thermal  
energy storage and dry cooling, *Environmental Science and Technology* 47, 2013.
- 24 37.Biencinto, M.a , González, L.a , Zarza, E.b , Díez, L.E.c , Muñoz-Antón, J., Performance  
model and annual yield comparison of parabolic-trough solar thermal power plants with either

- nitrogen or synthetic oil as heat transfer fluid, *Energy Conversion and Management* 87, 2014,  
2 238-249.
- 38.Kearney & Assoc. - Flabeg Solar International - KJC Operating Co. - Nextant (Bechtel) –  
4 NREL – Sandia Natl. Lab MWE, Engineering evaluation of molten salt HTF in a parabolic  
trough solar field, NREL Contract No. NAA-1-30441-04
- 6 39.Ravaghi-Ardebili Z., Manenti F., Corbetta M., Lima N.M.N., Zuniga Linan L., Papisidero  
D., 2013, Assessment of direct thermal energy storage technologies for concentrating solar  
8 power plants, *Chemical Engineering Transactions*, 35, 547-552
- 40.Antoni Gil, Marc Medrano, Ingrid Martorell, Ana Lázaro, Pablo Dolado, Belén Zalba,  
10 Luisa F. Cabeza, State of the art on high temperature thermal energy storage for power  
generation. Part 1—Concepts, materials and modellization, *Renewable and Sustainable*  
12 *Energy Reviews*, 14-1, 2010, 31-55
- 41.Zhen Yang, Suresh V. Garimella, Cyclic operation of molten-salt thermal energy storage in  
14 thermoclines for solar power plants, *Applied Energy*, 103, 2013, 256-265,
- 42.Carlos M. Fernández Peruchena, Lourdes Ramírez, Manuel A. Silva-Pérez, Vicente Lara,  
16 Diego Bermejo, Martín Gastón, Sara Moreno-Tejera, Jesús Pulgar, Juan Liria, Sergio Macías,  
Rocío Gonzalez, Ana Bernardos, Nuria Castillo, Beatriz Bolinaga, Rita X. Valenzuela, Luis F.  
18 Zarzalejo, A statistical characterization of the long-term solar resource: Towards risk  
assessment for solar power projects, *Solar Energy*, 123, 2016, 29-39
- 20 43.Romero, M., Marcos, M. J., Osuna, R., & Fernandez, V. (2000). Design and implementation  
plan of a 10 MW solar tower power plant based on volumetric-air technology in Seville  
22 (Spain). *Solar Engineering*, 89-98.
- 44.[www.ees.es/](http://www.ees.es/)
- 24 45.[www.mathworks.com](http://www.mathworks.com)
- 46.PVGIS <http://re.jrc.ec.europa.eu/pvgis/>

47. Chacartegui R. et al. Simplified Dynamic Models of a Concentrating Solar Tower Plant  
2 With a Heat Storage Tank. Comunicación en congreso. 6th SDEWES conference., Dubrovnik  
(Croacia). 2011
- 4 48. G. Angelino, P.C. Di Paliano, Multicomponent working fluids for organic Rankine cycles  
(ORCs), Energy Vol. 23, No. 6, pp. 449–463, 1998
- 6 49. F.J. Fernández, M.M. Prieto, I. Suárez, Thermodynamic analysis of high-temperature  
regenerative organic Rankine cycles using siloxanes as working fluids, Energy 36, 2011, 5239-  
8 5249.
50. B. Liu, K. Chien, C. Wong, Effect of working fluids on ORC for waste heat recover, Energy  
10 (2004) 1207-1217
51. Lai, M. Wenderland, J Fisher, Working fluids for high-temperature organic Rankine cycles,  
12 Energy (2011) 199-211.
52. U. Drescher, D. Bruggeman, Fluid selection for the ORC in biomass power and heat  
14 plants, Applied Thermal Energy (2007).
53. E. Prabhu, Solar Trough Organic Rankine Electricity System (STORES) Stage 1. Power  
16 Plant Optimization and Economics. NREL/SR-550-39433, March 2006
54. Chacartegui, R., Sanchez, D., Jimenez-Espadafor, F., Munoz, A., & Sanchez, T. (2008,  
18 January). Analysis of intermediate temperature combined cycles with a carbon dioxide topping  
cycle. In ASME Turbo Expo 2008: Power for Land, Sea, and Air (pp. 673-680). American  
20 Society of Mechanical Engineers.
55. Chacartegui R., Sánchez D., J. M. Muñoz, T. Sánchez, Alternative ORC bottoming cycles  
22 for combined cycle power plants, Applied Energy 86 (2009) 2162-2170.
56. Therminol VP-1 Data sheet, SOLUTIA, [www.solutia.com](http://www.solutia.com)
- 24 57. Daniel M. Blake, Luc Moens, Mary Jane Hale, Henry Price, David Kearney, and Ulf  
Herrmann, New Heat transfer and storage Fluids for parabolic trough solar thermal electric

- plant, Proceedings of the 11th SolarPACES International Symposium On concentrating Solar  
2 Power and Chemical Energy Technologies, 2002, Zurich, Switzerland.
58. James E. Pacheco, Steven K. Showalter, William J. Kolb, Development of a molten salt  
4 thermocline thermal storage system for parabolic trough plants, Proceedings of Solar Forum  
2001 Solar Energy: The Power to Choose April 21-25, 2001, Washington, DC.
- 6 59. A Gil, M. Medrano, I. Martorelli, A. Lazaro, P. Dolado, B. Zalba, L. Cabeza. State of the  
art on high temperature thermal energy storage for power generation. Part 1—Concepts,  
8 materials and modellization. *Renewable and Sustainable Energy Reviews* 14 (2010) 31–55.
60. Antonio Rovira, María José Montes, Manuel Valdes, José María Martínez-Val, Energy  
10 management in solar thermal power plants with double thermal storage system, *Applied  
Energy* 88 (2011) 4055–4066
- 12 61. SkyTrough, Next-generation solar parabolic trough technology.
62. Salvador Izquierdo, Carlos Montanes, Cesar Dopazo, Norberto Fueyo, Analysis of CSP  
14 plants for the definition of energy policies: The influence on electricity cost of solar multiples,  
capacity factors and energy storage, *Energy Policy* 38 (2010) 6215–6221.
- 16 63. R. Shankar Subramanian, *Shell-and-Tube Heat Exchangers*
64. A L Ling, *Heat Exchanger Selection and Sizing (Engineering Design Guideline)*, KLM,  
18 2008
65. Luong, D., & Tsao, T. C. (2015, October). Control of a Base Load and Load-Following  
20 Regulating Organic Rankine Cycle for Waste Heat Recovery in Heavy-Duty Diesel  
Powertrain. In *ASME 2015 Dynamic Systems and Control Conference* (pp. V001T12A002-  
22 V001T12A002). American Society of Mechanical Engineers.
66. Boissieux, X., Heikal, M. R., & Johns, R. A. (2000). Two-phase heat transfer coefficients  
24 of three HFC refrigerants inside a horizontal smooth tube, part II: condensation. *International  
Journal of Refrigeration*, 23(5), 345-352.

67.Incoprera, DeWitt, Bergman, Lavine, Fundamentals of heat and mass transfer

2 68.Lizarraga-Garcia, E., Mitsos, A., Effect of heat transfer structures on thermoeconomic performance of solid thermal storage, Energy 68, 2014, 896-909.

4 69.Flueckiger, S.M., Iverson, B.D., Garimella, S.V., Economic optimization of a concentrating solar power plant with molten-salt thermocline storage, Journal of Solar Energy Engineering, Transactions of the ASME 136, 2014.

6 70.Zhang Shengjun, Wang Huaixin, Guo Tao, Performance comparison and parametric optimization of subcritical Organic Rankine Cycle (ORC) and transcritical power cycle system for low-temperature geothermal power generation, Applied Energy 88 (2011) 2740–2754.

8 71.Maciej Lukawski, Design and optimization of standardized Organic Rankine Cycle Power Plant for European Conditions, Master Thesis, University of Iceland, 2009.

10 72.G. Glatzmaier, Developing a Cost Model and Methodology to Estimate Capital Costs for Thermal Energy Storage, NREL/TP-5500-53066 December 2011.

12 73.Price, H. (2003). Assessment of parabolic trough and power tower solar technology cost and performance forecasts. National Renewable Energy Laboratory, Golden, CO.

14 74.Kearney, D., Herrmann, U., Nava, P., Kelly, B., Mahoney, R., Pacheco, J., ... & Price, H. (2003). Assessment of a molten salt heat transfer fluid in a parabolic trough solar field. Journal of solar energy engineering, 125(2), 170-176.

16

18

## Tables captions

- 2  
Table 1: ORC Working fluids properties
- 4 Table 2: HTF and storage media properties  
Table 3. Heat transfer correlations used for heat exchangers models
- 6 Table 4: Power plant main assumptions  
Table 5. Influence of condensation pressure on Toluene's heat exchangers design
- 8 Table 6. ORC costs, efficiencies and mass flow (5 MWel plant)  
Table 7. PTC/ORC design conditions (5 MWel plant)
- 10 Table 8: Direct system and Indirect System – Discharging phase  
Table 9: Cost evaluation coefficients
- 12 Table 10: Global costs of main elements  
Table 11: Effect of Superheating in the costs of the plant
- 14 Table 12: Optimum LEC results as function of storage capacity  
Table 13. Summary of Indirect/Direct TES parabolic trough plant with Toluene as working  
16 fluid data

## Figures captions

- 2 Figure 1. PTC/ORC CSP power plants: two tanks direct (a and c) and indirect (b and d) thermal energy storage (TES) system. Direct system: HTF Hitec XL, Storage Medium: Hitec XL.
- 4 Indirect system HTF: Therminol VP-1, Storage Medium: Hitec XL
- Figure 2. Direct normal irradiance monthly patterns used for the analyses (left) and CSP plant location (right)
- 6
- Figure 3: Power block efficiency as function of the evaporation temperature for recuperative and non-recuperative cycles (left). Condensation temperature effect on recuperative efficiency (right).
- 8
- 10 Figure 4: Intermediate HE T-Q diagrams for Toluene (top) Cyclohexane (middle) and D4 (bottom)
- 12 Figure 5. Thermal Energy Storage System Costs
- Figure 6. ORCs evaporation temperatures and pressures as function of power plant load
- 14 Figure 7. Power block efficiency (left) and efficiency/rated capacity efficiency rate (right) at partial load
- 16 Figure 8. Solar Multiple Effect on LEC for different storage capacities. TES indirect system (left). TES direct system (right).
- 18 Figure 9. Electricity production, plant cost and LEC as function of SM. TES indirect system (left). TES direct system (right).
- 20 Figure 10. Annual electricity production as function of SM (above). Plant investment cost as function of SM (below). TES indirect system (left). TES direct system (right).

22

## Tables

24

Table 1: Properties of ORC Working fluids analyzed

26

Fluid	T <sub>crit</sub> (K)	P <sub>crit</sub> (bar)	T <sub>max</sub> (K)	P <sub>max</sub> (bar)
-------	-----------------------	-------------------------	----------------------	------------------------

Refrigerants/ hydrocarbons	<b>Toluene</b>	591.7	41.26	569	31.16
	<b>Cyclohexane</b>	553.6	40.75	536	32.67
	<b>n-hexane</b>	507.9	30.58	491	26.63
	<b>Isopentane</b>	460.4	33.70	448	27.87
	<b>n-Butane</b>	425.0	37.96	402	25.82
	<b>Isobutane</b>	407.8	36.40	380	22.50
Siloxanes/Abrev	<b>Hexamethyldisiloxane</b> (C <sub>6</sub> H <sub>18</sub> OSi <sub>2</sub> ) MM	518.0	19.3	513	17.65
	<b>Octamethyltrisiloxane</b> (C <sub>8</sub> H <sub>24</sub> Si <sub>3</sub> O <sub>2</sub> ) MDM	564.5	14.4	561	13.75
	<b>Decamethyltetrasiloxane</b> (C <sub>10</sub> H <sub>30</sub> Si <sub>4</sub> O <sub>3</sub> ) MD <sub>2</sub> M	599.5	12.3	597	11.88
	<b>Dodecamethylpentasiloxane</b> (C <sub>12</sub> H <sub>36</sub> Si <sub>5</sub> O <sub>4</sub> ) MD <sub>3</sub> M	629.0	9.5	627	9.28
	<b>Tetradecamethylhexasiloxane</b> (C <sub>14</sub> H <sub>42</sub> O <sub>5</sub> Si <sub>6</sub> ) MD <sub>4</sub> M	653.0	8.7	653	8.02
	<b>Dodecamethylcyclohexasiloxane</b> (C <sub>12</sub> H <sub>36</sub> Si <sub>6</sub> O <sub>6</sub> ) D <sub>6</sub>	645.0	9.6	645	9.51
	<b>D4</b> ((CH <sub>3</sub> ) <sub>2</sub> SiO) <sub>4</sub>	313,4	13,32	340,0	

2

4

Table 2: HTF and storage media properties

		<b>Therminol VP-1</b>	<b>Hitec XL</b>
<b>Freezing point</b>	[°C]	13	120
<b>Max applicable T</b>	[°C]	400	>500
<b>Density (@ 300°C)</b>	[kg/m <sup>3</sup> ]	815	1992
<b>Specific Thermal capacity C<sub>p</sub></b> <b>(@ 300°C)</b>	[J/kgK]	2319	1447

6

2

Table 3. Heat transfer correlations used for heat exchangers models

Circular tube-internal flow	$Nu_D = \frac{(f/8)(Re - 1000)Pr}{1 + 12.7(f/8)^{1/2} \left( Pr^{2/3} - 1 \right)}$	Gnielinski (20)	Economizer; Super-heater; Regenerator ; Oil-to-salt heat exchanger
	$f = (0.790 \log(Re) - 1.64)^{-2}$	Petukov (21)	
Cross flow - external flow	$Nu = C Re^m Pr^{1/3}$	Hilpert (22)	Economizer
Correlation for stratified flow	$\bar{h} = 0.555 \left( \frac{g \rho_l (\rho_l - \rho_v) h'_{gl} k_l^3}{\mu_l (T_{sat} - T_s) D} \right)^{1/4}$	Akers, Deans and Crosser (22)	Organic fluid at the condenser
	$h'_{gl} = h_{gl} + \frac{3}{8} c_{p,l} (T_{sat} - T_s) \quad Re_v \leq 35000$	(23)	
	$Ge = G(1 - x) + Gx \left( \frac{\rho_l}{\rho_v} \right)^{1/2}$ $Re = \frac{GeD}{\mu_l} \quad h = C Re^n Pr_l^{1/3} \quad Re_v > 35000$	(24)	
Saturated flow boiling region in smooth circular tubes	$\frac{h}{h_{sp}} = 0.6683 \left( \frac{\rho_l}{\rho_v} \right)^{0.1} \bar{X}^{0.16} (1 - \bar{X})^{0.64} f(Fr)$ $+ 1058 \left( \frac{q_s}{\dot{m}'' h_{gl}} \right)^{0.7} (1 - \bar{X})^{0.8} G_{s,f}$	(25)	Evaporator

4

6

8

2

Table 4: Power plant main assumptions

Hypothesis	Value
<b>Tmax (T8-solar field outlet)</b>	400°C
<b>Minimum <math>\Delta T</math> in heat exchangers</b>	10°C
<b>Net electric power Wel</b>	1-10 MW
<b><math>\eta_{is}</math> turbine</b>	0.85
<b><math>\eta_{is}</math> pump</b>	0.80
<b>Condenser water Inlet temperature</b>	10°C
<b>Toluene Maximum Temperature</b>	308.6 °C
<b>Cyclohexane Maximum Temperature</b>	270.3 °C
<b>Siloxane D4 Maximum Temperature</b>	303.4 °C
<b>Therminol VP-1 T<sub>sat</sub>, C<sub>p</sub>, H</b>	Manufacturer Data sheet
<b>Collector Area</b>	Manufacturer Data sheet

4

6

Table 5. Influence of condensation pressure on Toluene's heat exchangers design

Toluene								
Tcond [°C]	35	40	45	50	55	60	65	70
<b>pcond [kPa]</b>	6,20	7,84	9,82	12,21	15,06	18,43	22,40	27,04
<b><math>\eta</math> [%]</b>	30,5	29,9	29,2	28,6	28,0	27,3	26,8	26,1
<b>Ureg [W/m<sup>2</sup> k]</b>	21	25	30	35	42	50	59	69
<b>Ucond [W/m<sup>2</sup> k]</b>	1394	1366	1345	1330	1317	1307	1298	1290
<b>Mass flow [Kg/s]</b>	26,1	27,0	28,1	29,1	30,2	31,4	32,7	34,0
<b>PB cost [€/kW]</b>	1121	1076	1022	991	907	846	816	778

8

10

Table 6. ORC costs, efficiencies and mass flow (5 MW<sub>el</sub> plant)

	Tcond [°C]	Pcond [bar]	Teva [°C]	Peva [bar]	T3 [°C]	Mass flow [kg/s]	$\eta$ PB [%]	Cost PB [€/kW]
Toluene	55	0.151	302	33.5	367	24.3	31.5	825
Cyclohexane	40	0.245	255	29.5	285	29.1	28.7	933
D4	87	0.049	302	11.2	337	74.8	23.4	1088

12

2

Table 7. PTC/ORC design conditions (5 MW<sub>el</sub> plant)

		T <sub>5</sub> [°C]	T <sub>6</sub> [°C]	T <sub>7</sub> [°C]	T <sub>8</sub> [°C]	T <sub>9</sub> [°C]	HTF mass flow [kg/s]	ORC mass flow [kg/s]	η plant
Indirect	Toluene	217.7	217.7	218.1	400	400	34.8	24.3	23.3%
	Cyclohexane	141.7	141.7	141.9	400	400	27.03	29.1	21.6%
	D4	238.1	238.1	238.6	400	400	52.62	74.8	17.3%
Direct	Toluene	220.9	220.9	221.2	400	400	61.61	24.3	23.3%
	Cyclohexane	200	200	200.2	400	400	60.29	29.1	21.3%
	D4	238.1	238.1	238.5	400	400	91.85	74.8	17.3%

4

6

Table 8: Direct system and Indirect System – Discharging phase

	Direct system – Discharging phase			Indirect system – Discharging phase							
	T <sub>HOT TANK</sub> T <sub>9</sub> [°C]	T <sub>COLD TANK</sub> T <sub>5</sub> [°C]	HitecXL mass Flow [kg/s]	T <sub>9</sub> [°C]	T <sub>5</sub> [°C]	T <sub>11</sub> [°C]	T <sub>10</sub> [°C]	T <sub>HOT TANK</sub> T <sub>12</sub> [°C]	T <sub>COLD TANK</sub> T <sub>13</sub> [°C]	Thermino I VP-1 mass flow [kg/s]	Hitec XL mass flow [kg/s]
Toluene	400	221	61.61	38	239,	239,	38	390	250	45.09	77.90
Cyclohexan	400	200	60.29	38	141,	141,	38	390	200	29.29	63.12
D4	400	238	91.85	38	238,	238,	38	390	250	59.96	104.7

8

10

Table 9: Cost evaluation coefficients

K <sub>1</sub>	K <sub>2</sub>	K <sub>3</sub>	C <sub>1</sub>	C <sub>2</sub>	C <sub>3</sub>	B <sub>1</sub>	B <sub>2</sub>	F <sub>M</sub>	CEPCI <sub>1996</sub>	CEPCI <sub>2014</sub>
3.2138	0.2688	0.07961	-	0.05025	0.01474	1.8	1.5	1.25	382	539.4/576.1

12

2

Table 10: Global costs of main elements

Cost of:	Price	Reference
<b>Turbine</b>	450 €/kW	[71]
<b>Solar field</b>	213 €/m <sup>2</sup>	[62]
<b>Hitec XL</b>	1.19 \$/kg	[38]
<b>Therminol VP-1</b>	2.2 \$/kg	[38]
<b>Storage</b>	20,1 \$/kWh <sub>t</sub>	[38]
<b>Indirect</b>	0.2*Plant cost	[12]

4

6

8

Table 11: Effect of Superheating in the costs of the plant

Effects of superheating – Toluene – T <sub>eva</sub> 302°C – 6h TES – SM=2		
$\Delta T_{SH}$ [°C]	0	65
<b>ORC Efficiency [%]</b>	28,0%	31,5%
<b>A<sub>Solar Field</sub> [m<sup>2</sup>]</b>	69053	61714
<b>Plant cost [€/kW]</b>	5638	5044
<b>Plant cost [M€]</b>	28.2	25.2
<b>Solar Field cost [M€]</b>	14.7	13.1
<b>TES cost [M€]</b>	4.3	3.7
<b>ORC cost [M€]</b>	4.5	4.1
<b>Cost reduction</b>	System	Global
<b>ORC</b>	9%	1,4%
<b>Solar Field</b>	11%	5,5%
<b>TES</b>	12%	1,8%

10

2

Table 12: Optimum LEC results as function of storage capacity

LEC [c€/kWh]	Storage Hours	No storage	2	3	4	5	6	7	8	9	10
	<b>SM</b>	1.25 - 1.5	1.5 ± 0.1	1.5 - 1.75	1.75 ± 0.1	1.75 - 2	2 ± 0.1	2 - 2.25	2 - 2.25	2.25 ± 0.1	2.25 - 2.5
<b>Indirect TES</b>	<b>Toluene</b>	16.79	16.03	16.05	16.02	16.07	16.13	16.17	16.25	16.30	16.36
	<b>Cyclohexane</b>	17.13	17.03	16.96	16.87	16.87	16.91	16.91	16.96	17.00	17.04
	<b>D4</b>	21.83	20.94	21.01	20.99	21.05	21.10	21.14	21.27	21.33	21.42
<b>Direct TES</b>	<b>Toluene</b>	-	17.12	17.07	17.03	16.99	17.01	16.99	17.02	17.00	17.05
	<b>Cyclohexane</b>	-	18.50	18.41	18.34	18.28	18.24	18.20	18.23	18.20	18.23
	<b>D4</b>	-	22.09	22.07	22.07	22.05	22.09	22.09	22.16	22.16	22.25

4

6

2

Table 13. Summary of Indirect/Direct TES parabolic trough plant with Toluene as working fluid data

4

Toluene – Indirect/Direct TES						
Storage hours	0	2	4	6	8	10
SM	1.25	1.5	1.75	2	2.25	2.5
Tanks volume [m <sup>3</sup> ]	0	331.5/263	663.0/526	994.5/789	1326.0/1052	1657.5/1315
Solar field area [10 <sup>4</sup> m <sup>2</sup> ]	3.84	4.62/4.6	5.39/5.37	6.17/6.13	6.95/6.9	7.72/7.67
Investment Cost [M€]	15.10	18.55/18.17	22.00/21.42	25.54/24.65	29.09/27.90	32.64/31.14
Investment cost [€/kW]	2956	3703/3634	4407/4282	5113/4931	5819/5580	6527/6229
% solar field	55.0	53.6/54.4	52.6/53.8	51.9/53.5	51.4/53.2	50.9/52.9
% TES	0	6.8/5.8	11.5/9.8	14.8/12.8	17.4/15.0	19.4/16.8
% Power block	28.4	22.9/23.2	19.3/19.7	16.6/17.1	14.6/15.1	13.0/13.6
Production [GWh/y]	12.59	16.46/14.93	19.62/17.7	22.56/20.41	25.41/23.07	28.20/25.69
U.F.(%)	28.8	37.6/34.1	44.8/40.4	51.5/46.6	58.0/52.7	64.4/58.7
Annuity [M€]	1.74	2.15/2.11	2.55/2.48	2.96/2.86	3.37/3.23	3.78/3.61
O&M [M€]	0.35	0.457/0.42	0.545/49	0.627/0.57	0.706/0.64	0.783/0.71
LEC [c€/kWh]	16.79	16.03/17.12	16.02/17.03	16.13/17.01	16.27/17.02	16.41/17.05

6

# Figures

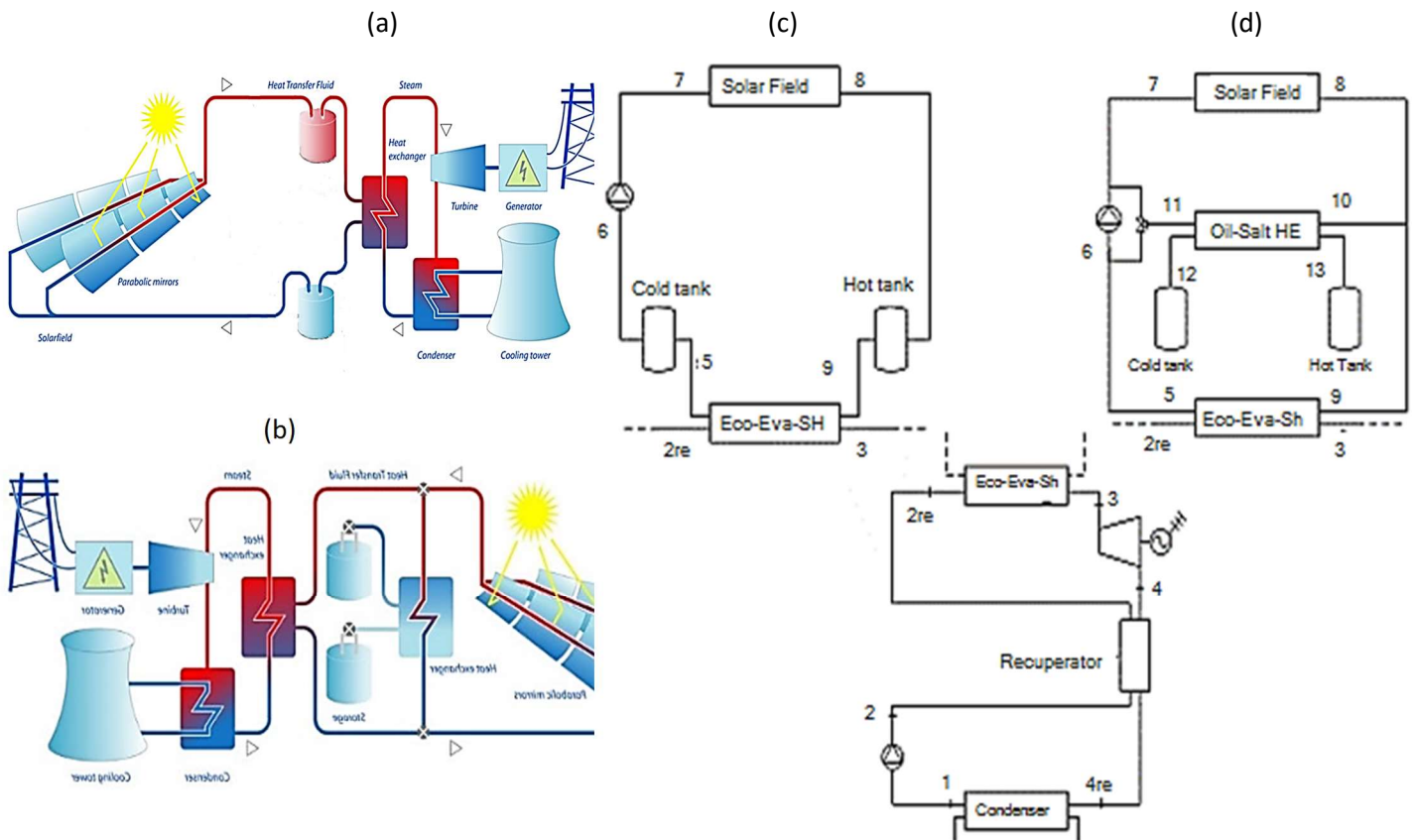


**Figure 1. PTC/ORC CSP power plant: two tanks direct (a and c) and indirect (b and d) thermal energy storage (TES) system. Direct system: HTF Hitec XL, Storage Medium: Hitec XL. Indirect system HTF: Therminol VP-1, Storage Medium: Hitec XL**



**Figure 2. Direct normal irradiance monthly patterns used for the analyses (left) and CSP plant location (right)**

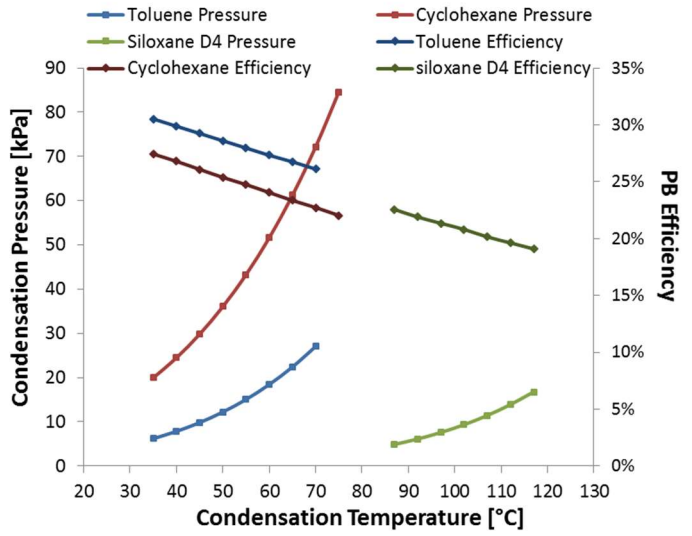
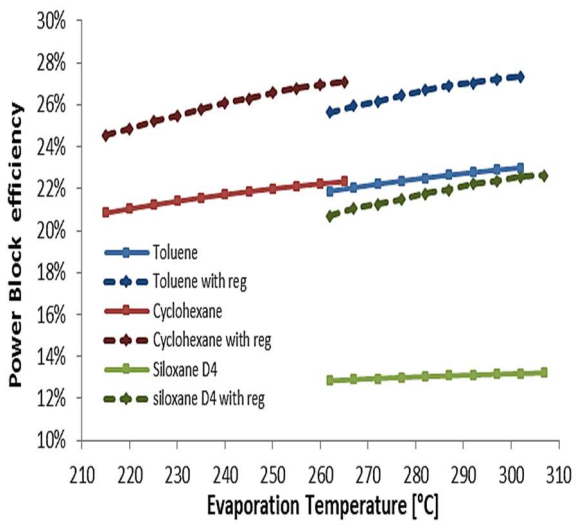


**Figure 3: Power block efficiency as function of the evaporation temperature for recuperative and non-recuperative cycles (left). Condensation temperature effect on recuperative cycle efficiency (right).**

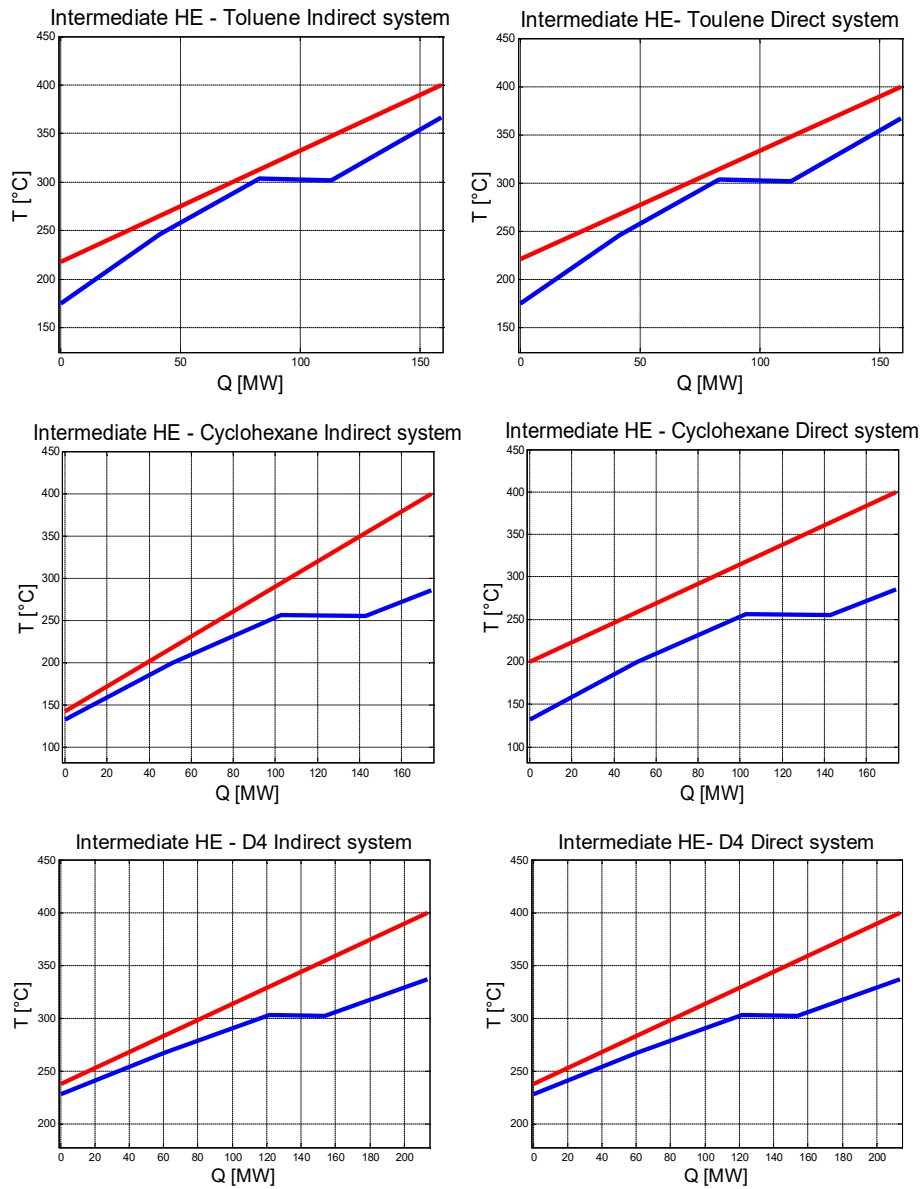


Figure 4: Intermediate HE T-Q diagrams for Toluene (top) Cyclohexane (middle) and D4 (bottom)

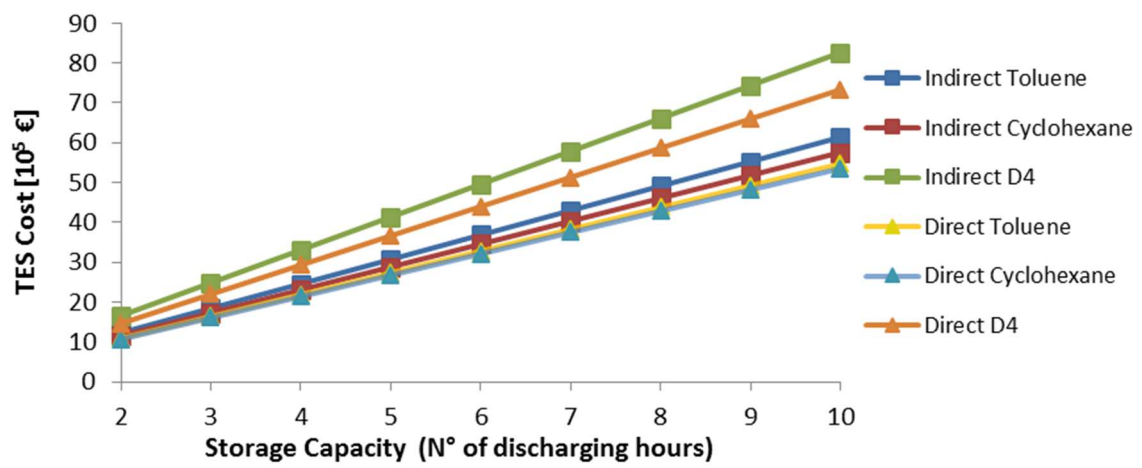


Figure 5. Thermal Energy Storage System Costs

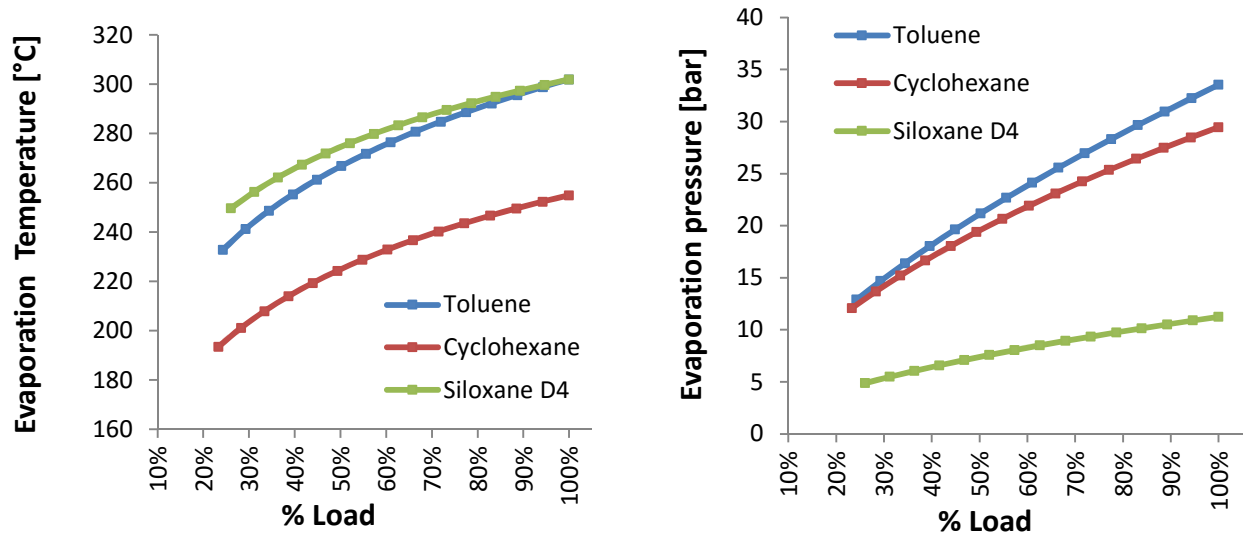


Figure 6. ORCs evaporation temperatures and pressures as function of power plant load

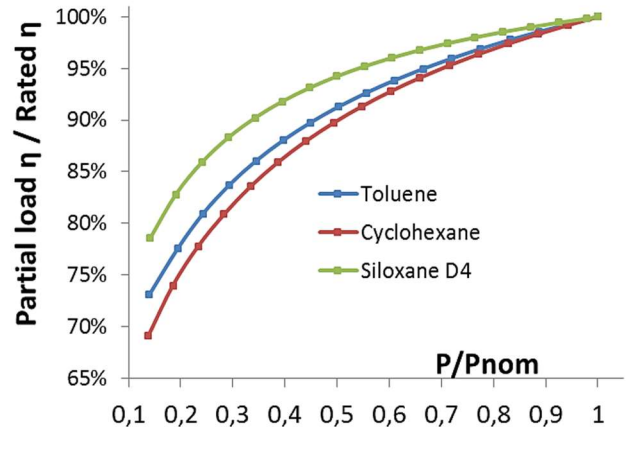
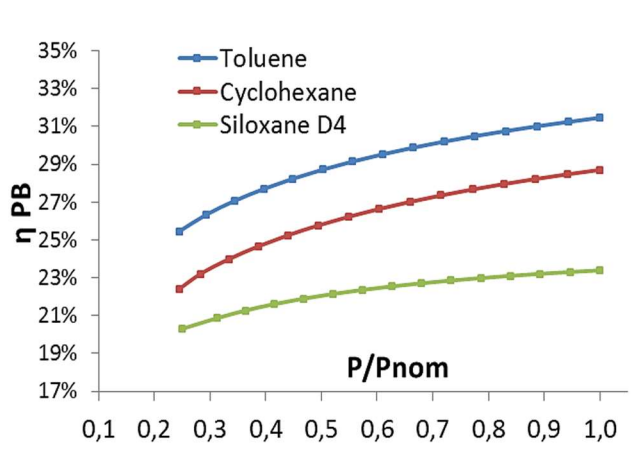


Figure 7. Power block efficiency and efficiency/rated capacity efficiency rate at partial load

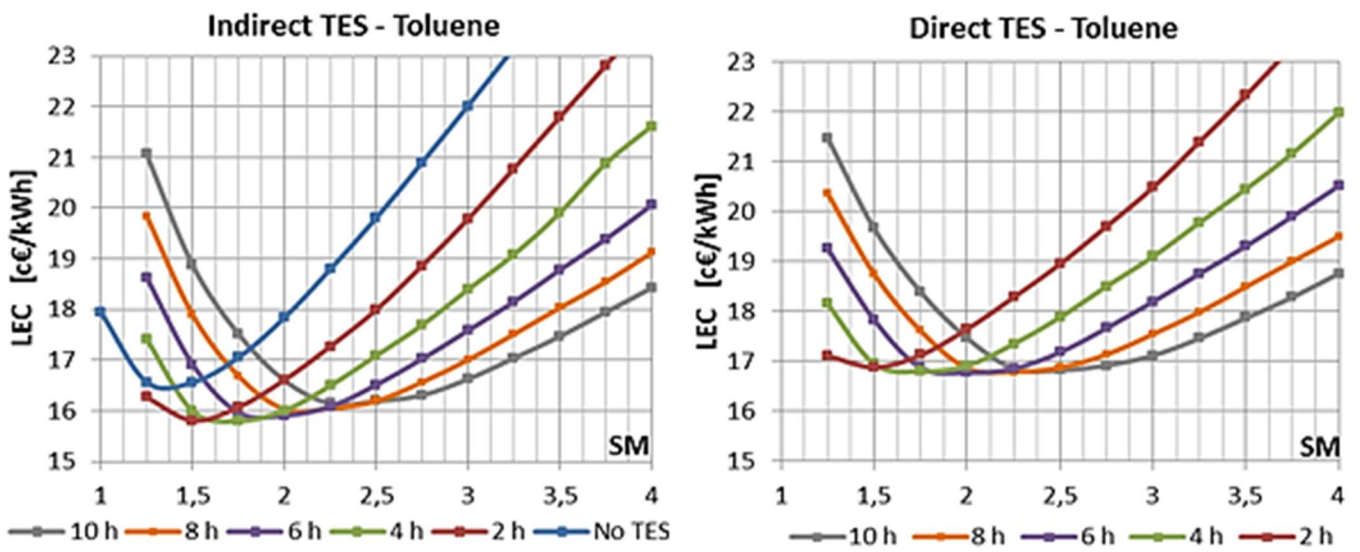


Figure 8. Solar Multiple Effect on LEC for different storage capacities. TES indirect system (left). TES direct system (right).

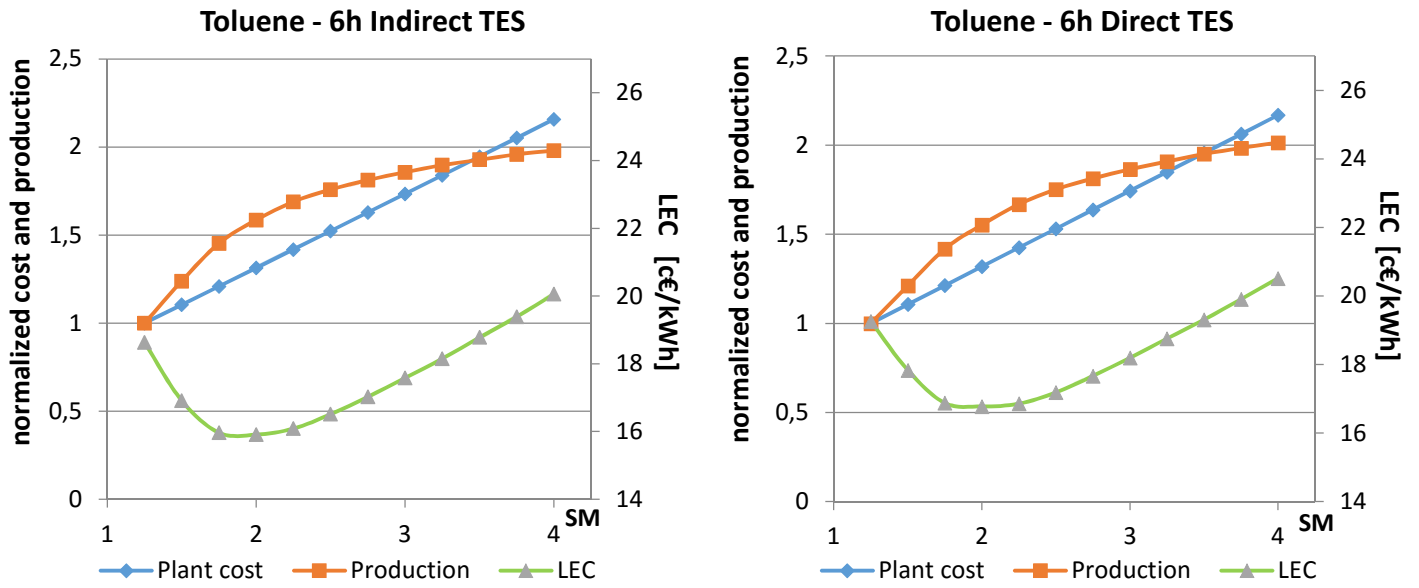


Figure 9. Electricity production, plant cost and LEC as function of SM. TES indirect system (left). TES direct system (right).

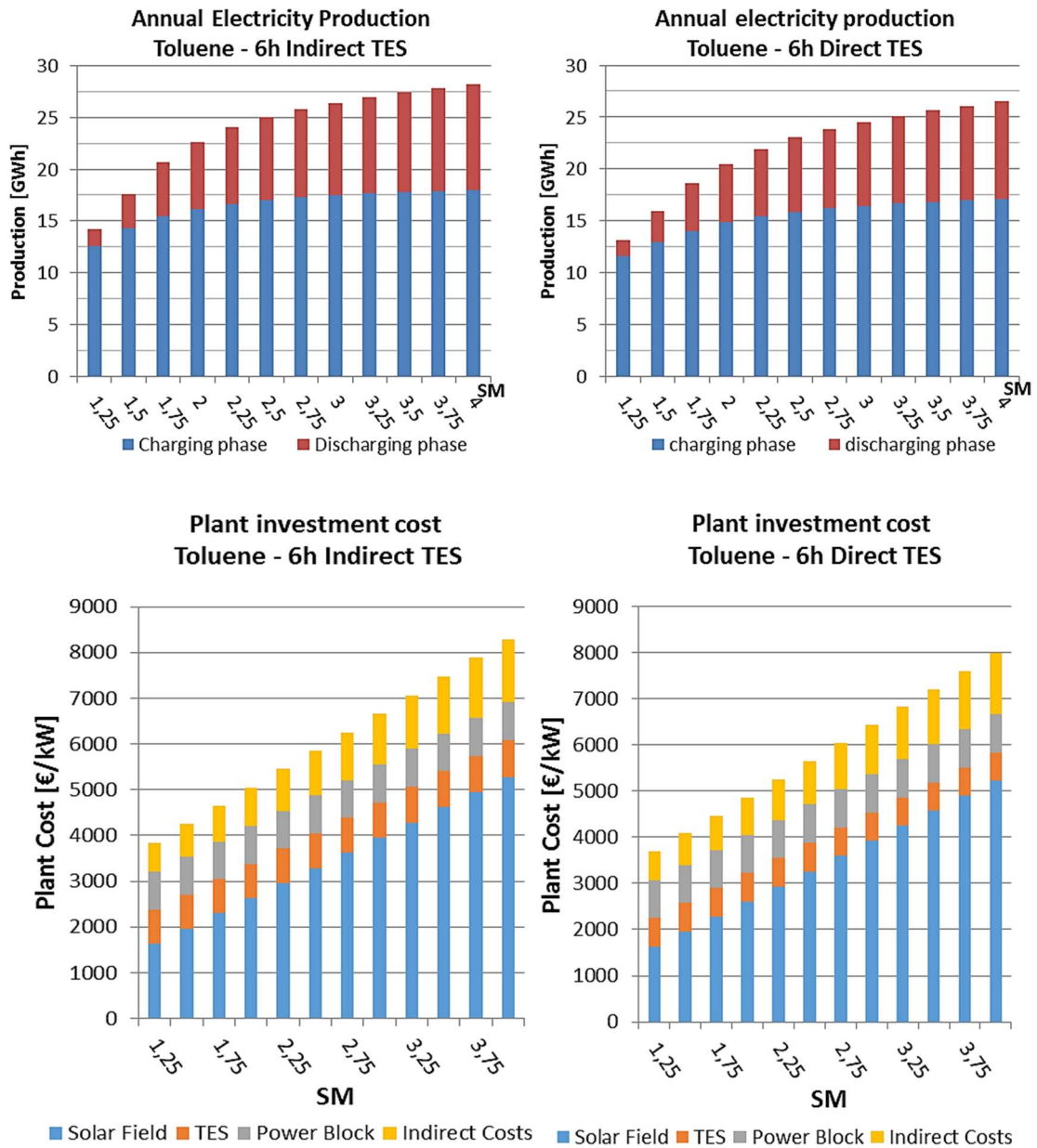


Figure 10. Annual electricity production as function of SM (above). Plant investment cost as function of SM (below). TES indirect system (left). TES direct system (right).